reactions were followed for changes of 0.5–2.0 A units (times of 1–36 h) and gave essentially linear changes in A with time for these periods. Second-order rate constants were obtained with eq 3 by substituting ϵ^{-1} dA for d[**3**] with the extinction coefficient ϵ for the particular acid.

For the conversion of **1** to **3** using Tobey's method[27] the initial concentration of **1** was 1–6 × 10^{-2} M. The reaction was carried out in 78.4% H_2SO_4. After 2–3 half-lives the absorbance readings were divided into two sets, A_1 and A_2, separated by a constant time interval. The plot of $A_1 - A_2$ vs. $t_2A_2 - t_1A_1$ was linear with slope k_2[**1**]. The rates agreed with those from the initial rates method to within ±5%.

For measurements of iodination rates stock solutions of **1** were added to sulfuric acid in the UV cell to give initial concentrations of 3–12.5 × 10^{-3} M. A solution of I_2 in ethanol was injected so that the initial I_2 concentration was no more than 10% of that of **1**. Addition of iodide gave a less stable absorption, so this was omitted. The decrease of the I_2 absorption with time was followed at 461 nm and gave linear plots for at least 95% reaction (r = 0.9999). The rates were calculated from the expression $-d[I_2]/dt = k_1[\mathbf{1}]$ or $k_1 = -(\epsilon[\mathbf{1}])^{-1}\, dA/dt$ where ϵ is the extinction coefficient measured for I_2 in the solution and dA/dt is the slope of the plot. Alternatively, **1** was added to I_2 generated from NaI and excess KIO_3. In this system,[29b,30d] each mol of **1** consumes 2.5 mol of I_2, so the rate expression is $k_1 = -(2.5\epsilon[\mathbf{1}])^{-1}\, dA/dt$. There was good agreement between the two methods.

In the reaction of unpurified **1** about 2 μL of the acetaldehyde was injected into the cuvette to give a 5 × 10^{-2} M solution, and the final A values indicated the formation of about 10^{-4} M **3**. In 87.5% H_2SO_4 the half-life for formation of **3** from unpurified **1** was 6 s (Table III), and in a 5 × 10^{-2} M solution of pure **1** the initial pseudo-first-order rate constant for formation of **3** from **1** in 88.2% acid would be 1.5 × 10^{-4} s^{-1} (Table II), or a half-life of 1 h. Thus the latter process would not interfere with measurement of the former.

Equilibrium constants for the interconversion of **2** and **3** (Table I) were calculated from the decrease in the absorption of **3** injected into the particular acid. There was no significant absorption due to **2**, and the rate of conversion was slow enough so that the fraction of **3** converted to **2** could be taken as $(A_0 - A)/A_0$, where A_0 and A are the initial and final absorbances.

In the stronger acids (88–96%) it was observed that the 256 nm λ_{max} of **3** shifted to a 254 nm maximum in a process whose first-order rate could be readily monitored. The rate of this process was lower in the stronger acids. This is probably due to a physical phenomenon of some sort, as no concomitant change in the ^1H NMR spectrum could be detected, but no specific assignment of this process has been made.

Acknowledgment. Valuable discussions with Professors A. Jerry Kresge and J. Peter Guthrie are gratefully acknowledged, as is the financial support of the Natural Sciences and Engineering Research Council of Canada.

Appendix 1. Steady-State Analysis of Enol Formation

In Scheme I, let $K_{SH^+} = k_{-4}/k_4$ and $K_H = k_{-5}/k_5$. Then

$$d[SH^+]/dt = k_4[S][H^+] + k_5[H][H_3O^+] - k_1[SH^+][H_2O]^2 - k_{-4}[SH^+] - k_{-5}[SH^+][H_2O]^2 = 0$$

$$d[E]/dt = k_1[SH^+][H_2O]^2 = k_1[H_2O]^2(k_4[S][H^+] + k_5[H] \times [H_3O^+])/(k_1[H_2O]^2 + k_{-4} + k_{-5}[H_2O]^2)$$

Now $k_4 \gg k_5$[36e] and $k_{-4} \gg k_{-5}$ and k_1, so this becomes

$$d[E]/dt = k_1[H_2O]^2k_4[S][H^+]/k_{-4} = (k_1/K_{SH^+})[S][H^+][H_2O]^2$$

which is the same equation previously obtained for enolization processes.[11] The rate depends on the actual concentration of free **1** present. This analysis applies to the aqueous standard state (for clarity the superscript zeroes are omitted here) and thus uses concentrations rather than activities. Since k_1 is the rate-determining step for enolization, it is assumed to be irreversible; enol is captured by iodine as soon as it is formed.

Appendix 2. Derivation of Rate Equation for Acetaldehyde Condensation

Using Scheme I, the observed second-order rate constants k_2 for the formation of **2** are given by

$$k_2C_S^2 = k_2^0a_{SH^+}a_Ea_w/f_*$$

Writing $K_E = a_S/a_E$ and $K_{SH^+} = a_Sa_{H^+}/a_{SH^+}$, this becomes

$$k_2C_S^2 = (k_2^0K_E/K_{SH^+})a_wC_S^2C_{H^+}(f_S^2f_{H^+}f_*)$$

We have[10]

$$\log(f_Sf_{H^+}/f_*) = m^* \log (f_Sf_{H^+}/f_{SH^+}) = m^*m^* \log (f_{B^*}f_{H^+}/f_{B^*H^+}) = m^*m^*X$$

Thus if the variation of f_S with acidity is small, the activity coefficient ratio should still be linear in X. On taking logs eq 4 results.

Registry No. **1**, 75-07-0; **2**, 107-89-1; **3**, 4170-30-3; **5**, 95764-57-1; vinyl alcohol, 557-75-5; hydrogen, 1333-74-0; ethyl 3-(trimethylsilyloxy)butyrate, 55816-59-6.

Host–Guest Complexation. 35. Spherands, the First Completely Preorganized Ligand Systems[1,2]

Donald J. Cram,* Takahiro Kaneda, Roger C. Helgeson, S. Bruce Brown, Carolyn B. Knobler, Emily Maverick, and Kenneth N. Trueblood

Contribution from the Department of Chemistry and Biochemistry, University of California at Los Angeles, Los Angeles, California 90024. *Received July 30, 1984*

Abstract: Spherands **1–5** and the related macrocycle **6** which are described in this paper are composed mainly of four to six aryloxy units attached to one another in such a way that the orbitals of the unshared electron pairs of their oxygens line an enforced cavity. These ligand systems strongly complex only Li^+ and Na^+ ions and reject K^+, Ca^{2+}, and Mg^{2+} ions. Their syntheses, representative crystal structures, and a qualitative survey of their binding properties are reported. The critical ring closures of these 18-membered-ring systems involved oxidations of appropriate bisaryllithiums with $Fe(acac)_3$ in refluxing benzene or THF to aryl radicals which coupled with one another—a reaction invented for construction of these hosts. The crystal structure of **1** clearly shows its unoccupied cavity lined with electron pairs. The crystal structures of **1**·LiCl and **1**·$NaCH_3SO_4$ indicate that no conformational reorganization of the host was involved in complexation. The crystal structures of the complexes of the polycyclic hosts **4**·$LiFeCl_4$ and **5**·LiCl show the ligating systems to be highly strained and to contain severe oxygen–oxygen compression.

Spherands are systems of ligands *organized prior to complexation* so that the orbitals of unshared electron pairs of the binding sites line a roughly spherical cavity enforced by a support structure of covalent bonds. Thus a spherand must be organized

0002-7863/85/1507-3645$01.50/0 © 1985 American Chemical Society

Chart I. Ligating Systems Arranged in Decreasing Order of Their Preorganization

spherands > cryptands > chorands > podands > solvents

for complexation during its synthesis rather than during its complexing act. Spherands must be rigid enough so that their parts cannot rotate to fill their own cavities, which ordinarily will be too small to be filled with either solvent or parts of solvent. Thus the cavity should be empty and relatively unsolvated. The crystal structures of a free spherand and the spherand part of its complexes should be very similar.

The spherands are at the end of a progression of ligand structures which vary in the extents to which the guest cations organize their own coordination shells (Chart I). Guest cations exert maximum organization when individual solvent molecules must be *collected* and *oriented* to solvate the ions. *Podands*[3] are acyclic *collections* of binding sites held together by appropriate spacer units. Thus the binding sites are collected prior to complexation, but during the complexing act many degrees of conformational freedom must be frozen out and the binding sites must be desolvated. *Chorands*[4] are cyclic, and *cryptands*[5] are polycyclic collections of binding sites which possess a variety of conformations, many of which fill their own potential cavities with their own spacer units, or with parts of solvent which solvate the binding sites. During complexation, guest cations develop cavities they can occupy by conformational reorganization and by desolvation of the binding sites of the host. The additional bridges of the cryptands, by decreasing the number of nonbinding conformations and by partially inhibiting solvation, put a smaller reorganization burden on the guest than do the chorands. Finally, the preorganized spherands[2] put no reorganizational and little host desolvation burden on the guest. Conversely, all hosts must desolvate the guests during complexation, the spherands and cryptands most thoroughly.

The tendencies of the chorands and cryptands to fill their own potential cavities with inward-turned methylene groups are illustrated by representations of the crystal structures of 18-crown-6[6] (A) and of [2.2.2]cryptand[7] (C) in Scheme I. The ability of K^+ as a guest to reorganize 18-crown-6 (A) in forming 18-crown-6·KSCN is shown by the crystal structure of the complex, B.[6] Likewise, K^+ reorganizes [2.2.2]cryptand (C) in forming [2.2.2]cryptand·KI, whose crystal structure is shown in D.[7] Many other examples of chorand host reorganizations by guests have been reported.[8]

The present paper reports the syntheses of the first four spherands and related compounds to be designed and prepared[2] (**1–6**), several of their complexes, five crystal structures of such compounds, and a qualitative survey of their complexing properties. In a companion paper, correlations are made between the structures of these spherands and their complexing power and with their rates of complexation–decomplexation.[9] In both papers, the principles of preorganization and of complementarity will be elaborated and developed.

Scheme I. Representations of Crystal Structures of a Chorand and a Cryptand and Their Complexes

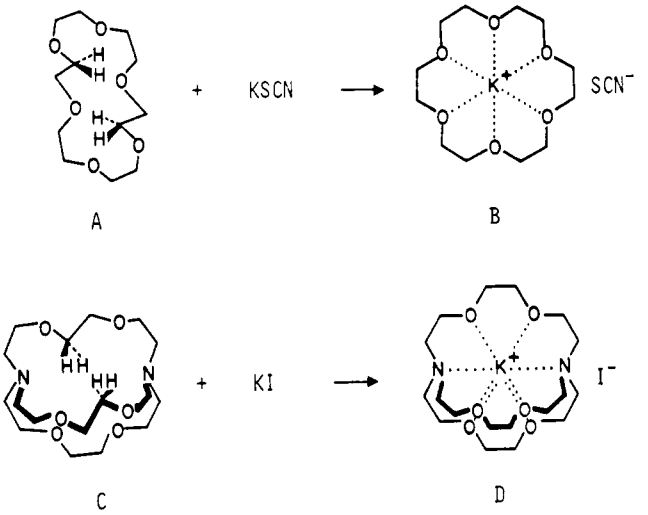

Results and Discussion

Design of the Spherands. At the outset of this work, we wished to design spherands that would provide extreme examples to test the validity of the self-evident principles of complementarity and preorganization. The principle of complementarity states that "in complexes of substantial stability, the binding sites of host and guest components must simultaneously contact and attract one another." The principle of preorganization states that "the more highly hosts and guests are organized for binding and for low solvation *prior* to their complexation, the more stable will be their complexes".[10] These principles are based on the presumption that the binding forces at each site are similar to those that involve solvation and ion-pairing, and therefore are very small compared to the forces of covalent bonds. Since we have defined host–guest complexes as "two or more molecules or ions held together in unique structural relationships",[11] the structuring of host–guest complexes depends on cooperativity between many contacting sites which because of their organization are able to compete with solvent.

Formulas **1–6** specify the connectedness, the configurations, and the conformations of all units except those defined by rotations about the CH_3– and CH_2–CH_2 bonds. The formulas provide little guidance as to potential nonbonded repulsions between the molecular parts, or bond angle strain, which in these crowded compounds are interdependent. Skeletal models of **1–6** suggest that bond angle strain is not high in the absence of atom-space occupation requirements. Only examination of Corey–Pauling–Koltun (CPK) molecular models of **1–6** provided guidance for the conception of these structures as spherands. These models were developed under the auspices of the National Institutes of Health, Education, and Welfare, the National Science Foundation, and the American Society of Biological Chemists "for constructing macromolecules of biological interest". They are based on crystal structures of biologically important compounds.[12] Scheme II outlines the connection between the structures of *biotic* compounds, CPK molecular models, molecular models of biotic systems, crystal

(1) We gratefully acknowledge support from the Division of Basic Sciences of the Department of Energy for the research on the design, synthesis, and binding properties of the spherands (D. J. Cram, T. Kaneda, R. C. Helgeson, and S. B. Brown) and from the National Science Foundation for that on the crystal structure determinations (K. N. Trueblood, E. Maverick, and C. B. Knobler).

(2) Some of these results have appeared as communications: (a) Cram, D. J.; Kaneda, T.; Helgeson, R. C.; Lein, G. M. *J. Am. Chem. Soc.* **1979**, *101*, 6752–6754. (b) Trueblood, K. N.; Knobler, C. B.; Maverick, E.; Helgeson, R. C.; Brown, S. B.; Cram, D. J. *Ibid.* **1981**, *103*, 5594–5596. (c) Cram, D. J.; Lein, G. M.; Kaneda, T.; Helgeson, R. C.; Knobler, C. B.; Maverick, E.; Trueblood, K. N. *Ibid.* **1981**, *103*, 6228–6232.

(3) Weber, E.; Vögtle, *Top. Current Chem.* **1981**, *98*, 3–41.

(4) Pederson, C. J. "Synthetic Multidentate Macrocyclic Compounds"; Izatt, R. M., Christensen, J. J., Ed.; Academic Press: New York, 1978; pp 1–52.

(5) Lehn, J.-M. *Struct. Bonding (Berlin)* **1973**, *16*, 1–69.

(6) (a) Dunitz, J. D.; Dobler, M.; Seiler, P.; Phizackerly, R. P. *Acta Crystallogr., Sect. B* **1974**, *B30*, 2733–2738. (b) Dunitz, J. D.; Seiler, P. *Ibid.* **1974**, *B30*, 2739–2741. (c) Dobler, M.; Dunitz, J. D.; Seiler, P. *Ibid.* **1974**, *B30*, 2741–2743. (d) Seiler, P.; Dobler, M.; Dunitz, J. D. *Ibid.* **1974**, *B30*, 2744–2746. (e) Dobler, M.; Phizackerley, R. P. *Ibid.* **1974**, *B30*, 2746–2747. (f) Dobler, M.; Phizackerley, R. P. *Ibid.* **1974**, *B30*, 2748–2750.

(7) (a) Weiss, R.; Metz, B.; Moras, P. D. *Proc. Int. Conf. Coord. Chem., 13th* **1970**, *2*, 85–86. (b) Metz, B.; Moras, D.; Weiss, R. *Acta Crystallogr., Sect. B* **1973**, *B29*, 1377–1381.

(8) Cram, D. J.; Trueblood, K. N. *Top. Current Chem.* **1981**, *98*, 43–106.

(9) Cram, D. J.; Lein, G. M. *J. Am. Chem. Soc.*, following paper in this issue.

(10) Artz, S. P.; Cram, D. J. *J. Am. Chem. Soc.* **1984**, *106*, 2160–2170.

(11) Kyba, E. P.; Helgeson, R. C.; Madan, K.; Gokel, G. W.; Tarnowski, T. L.; Moore, S. S.; Cram, D. J. *J. Am. Chem. Soc.* **1977**, *99*, 2564–2571.

(12) Koltun, W. L. *Biopolymers* **1965**, *3*, 665–679.

Scheme II. Molecular Design, Molecular Model, and Crystal Structure Connections

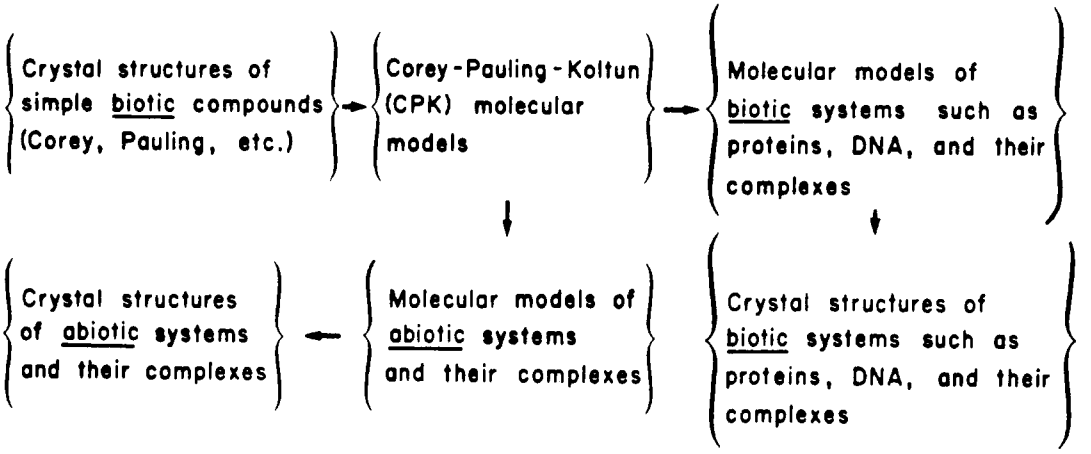

Chart II

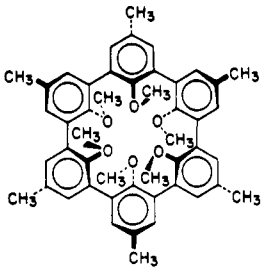

1, $A(AA)_2A$

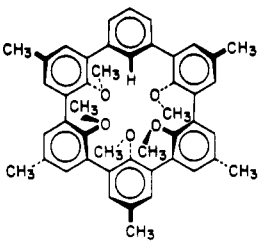

2, $A(AA)_2P$

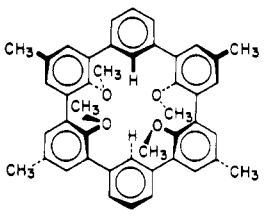

3, $P(AA)_2P$

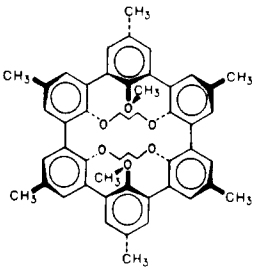

4, $[B(A)(M_3)B]_2$

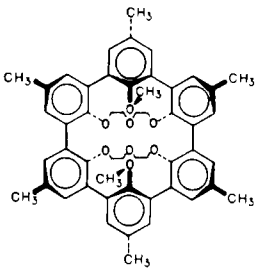

5, $[B(A)(EOE)B]_2$

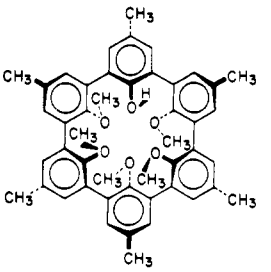

6, $A(AA)_2Ah$

structures of biotic systems, molecular models of *abiotic* compounds, and crystal structures of abiotic systems. The results of this paper particularly provide a test of the usefulness and limitations of CPK models as a means of designing host–guest complexes.

Models of **1**, **2**, **4**, and **5** indicate that the compounds contain enforced cavities lined with the orbitals of the unshared electron pairs of the oxygens, which in turn are covered with a hydrocarbon shell of methyl, methylene, and aryl groups. The unshared electron pairs are in an environment whose dielectric properties are between those of a vacuum and of a hydrocarbon. Furthermore, they are too deeply buried to be solvated. Thus complexation of these compounds should not involve much solvent reorganization involving the host.

We find it convenient to represent the hosts and their precursors with line formulas in which the orders of letters indicate the orders of attachment of the units. Chart III identifies the letters with the structures of the units. In the two polycyclic hosts, B serves as the bridgehead unit linked through their oxygens to M_3 or EOE units to transannular B units.

Syntheses. Starting compounds BrABr (**7**) and BrAABr (**8**)[13a] were available from prior studies.[13b] Oxidation of an aqueous solution of *p*-cresol with $FeCl_3$ provided HAhAhAhH (**9**, 20–40%),[13b,14] methylation of which gave HAAAH (**10**, 71%).[13b] Bromination of HAhAhAhH (**9**)[15] and methylation of the product produced BrAAABr (**11**, 85%). The Kumada cross-coupling[16] of 2-methoxy-5-methylphenylmagnesium bromide (HAMgBr) with 1,3-dibromobenzene ($NiCl_2$·$[P(C_6H_5)_3]_2$) gave HAPAH (**12**, 71%), which was demethylated and brominated to provide BrAhPAhBr (**13**, 85% overall). Methylation of this compound gave BrAPABr (**14**, 95%). Methylation of HAhAhAhH with CH_3I and 1 equiv of K_2CO_3 produced center-methylated product HAhAAhH (**15**, 72%), which was brominated to give BrAhAAhBr (**16**, 88%).[17a]

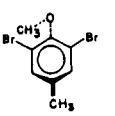

7, BrABr

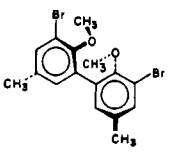

8, BrAABr

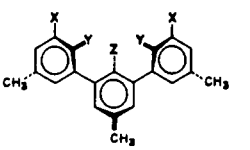

9, HAhAhAhH, X = H, Y = Z = OH
10, HAAAH, X = H, Y = Z = OCH_3
11, BrAAABr, X = Br, Y = Z = OCH_3
12, HAPAH, X = Z = H, Y = OCH_3
13, BrAhPAhBr, X = Br, Y = OH, Z = H
14, BrAPABr, X = Br, Y = OCH_3, Z = H
15, HAhAAhH, X = H, Y = OH, Z = OCH_3
16, BrAhAAhBr, X = Br, Y = OH, Z = OCH_3

The critical oligomeric macrocyclizations of **7**, **8**, **10**, and **11** to give $A(AA)_2A$·LiCl (**1**·LiCl) involved invention of a new re-

(13) (a) Koln, M.; Segel, A. *Monatsh. Chem.* **1925**, *46*, 661–669. (b) Koenig, K. E.; Lein, G. M.; Stückler, P.; Kaneda, T.; Cram, D. J. *J. Am. Chem. Soc.* **1979**, *101*, 3553–3566.
(14) Bowden, K.; Reece, C. R. *J. Chem. Soc.* **1950**, 2249.
(15) Bacon, R. G. R.; Grime, R. G.; Munro, D. J. *J. Chem. Soc.* **1954**, 2275–2280.
(16) Tumeo, K.; Sumitani, K.; Kiss, Y.; Semdayashi, M.; Fujioka, A.; Kodama, S.; Nakajima, I.; Minato, A.; Kumada, M. *Bull. Chem. Soc. Jpn.* **1976**, *49*, 1958–1969.
(17) (a) Lein, G. M.; Cram, D. J. *J. Am. Chem. Soc.* **1985**, *107*, 448–455. (b) Artz, S. P.; deGrandpre, M. P.; Cram, D. J. *J. Org. Chem.* **1985**, *50*, 1486.

Chart III

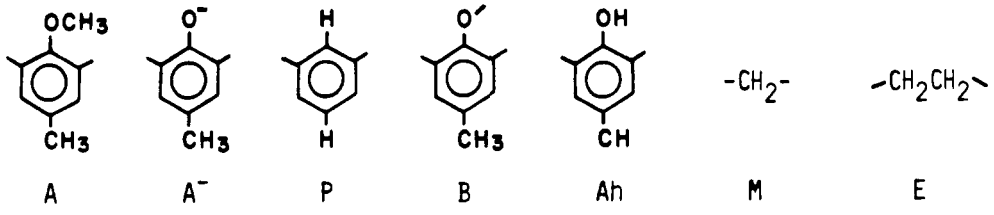

Table I. Distances and Angles in Crystal Structures of A(AA)$_2$A (**1**) and Complexes

structural parameters	1	1·LiCl	1·NaSO$_4$CH$_3$
Distances (Å)			
hole diameter	1.62	1.48	1.75
O to O, pseudoortho	2.92	2.78	3.00
O to O, pseudometa	3.32	3.24	3.43
O to O, pseudopara	4.42	4.28	4.55
O to plane of attached aryl[a]	0.20	0.07	0.12
C to plane of attached aryl[b]	0.16[c]	0.16[c]	0.16
Angles (deg)			
aryl folds on O–Ar–CH$_3$ axis	6.3	2.6	4.8
Ar–Ar planes (dihedral)[d]	52	56	61
C–O–C planes and aryl planes[e]	62	85	84
Ar–O–CH$_3$[f]	115	112	113

[a] O's are bent out of best planes of their attached aryls. [b] C's of attached aryls are bent out of best planes of their reference aryls. [c] Average values for all aryl rings. [d] Best plane dihedral angles. [e] Best aryl planes. [f] Normal angle is 118°.

action. A wide variety of oxidations of arylorganometallic reagents to give coupled radicals were studied, the best of which turned out to be the reaction of aryllithium reagents with Fe(acac)$_3$. The reaction is compatible with those groups in whose presence aryllithiums can be prepared, and the yields can be as high as 95%. Dilithiation with *sec*-butyllithium of BrABr (**7**), of BrAABr (**8**), or of BrAAABr (**11**) at −78 °C in THF followed by oxidation of the organometallics with Fe(acac)$_3$ in benzene led to the respective yields of 2.9, 7.5, and 28% for A(AA)$_2$A·LiCl (**1**·LiCl). As expected, the yields increased as the number of bonds being formed decreased. This generalization broke down when Br(A)$_6$Br (**19**) was submitted to the same reaction to give **1**·LiCl in 18% yield. We attribute this lower yield to difficulties in adding the gelatin-like mixture of the derived Li(A)$_6$Li in THF to the benzene mixture of Fe(acac)$_3$, a problem not encountered in the other ring closures. Compound **19** was prepared by FeCl$_3$ oxidation of H(Ah)$_3$H (**9**) in CH$_3$CN–H$_2$O to give H(Ah)$_6$H (**17**, 48%), which was brominated to provide Br(Ah)$_6$Br (**18**, 99%), methylation of which produced Br(A)$_6$Br (**19**, 50%).

Cyclic A(AA)$_2$A·LiCl (**1**·LiCl) was also obtained (17%) when HAAAH (**10**)[13b] was metalated directly in Et$_2$O in the presence of LiBr (generated in situ from (CH$_3$)$_3$CBr and BuLi), and the lithiated product was oxidized with Fe(acac)$_3$ in benzene. In the absence of added or generated LiBr, the yield decreased to 5%. We believe the aryllithiums produced in these reactions are oxidized to aryl radicals that undergo aryl–aryl coupling reactions.

The A(AA)$_2$A·LiCl complex (**1**·LiCl) was decomplexed (84%) by heating that material in 4:1 methanol–water at 125 °C for 20 days, the reaction being driven by the crystallization (phase transfer) of free **1** from the medium, in which it is very insoluble. Lithiation and oxidative cross-coupling of 1 mol of BrAAABr (**11**) with 4 mol of BrAPABr (**14**) gave 6% of A(AA)$_2$P (**2**) and homocoupled products A(AA)$_2$A·LiCl (**1**·LiCl, 9%) and P(AA)$_2$P (**3**, 12%).

The bridged spherands were prepared as follows. Treatment of diphenol BrAhAAhBr with Br(M$_3$)Br–KI–K$_2$CO$_3$ in acetone and with TsOEOEOTs–KOH in THF gave BrB(A)(M$_3$)BBr (**20**, 44%) and BrB(A)(EOE)BBr (**21**, 84%), respectively. When lithiated and oxidized, BrB(A)(M$_3$)BBr (**20**) gave [B(A)(M$_3$)B]$_2$·LiCl (**4**·LiCl, 13%), which was decomplexed by heating in water–pyridine at 100 °C to give [B(A)(M$_3$)B]$_2$ (**4**, 66%). The decomplexation was driven by crystallization of the free ligand system. When lithiated and oxidized, BrB(A)(EOE)BBr (**21**) provided [B(A)(EOE)B]$_2$·LiCl (**5**·LiCl, 6%), which was decomplexed by heating in water–methanol at 125 °C to provide [B(A)(EOE)B]$_2$ (**5**, 79%). Again, the decomplexation was driven by crystallization of the free ligand from the solvent.

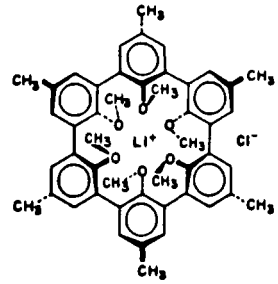

A(AA)$_2$A·LiCl (**1**·LiCl)

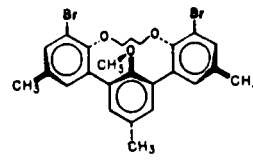

BrB(A)(M$_3$)BBr (**20**)

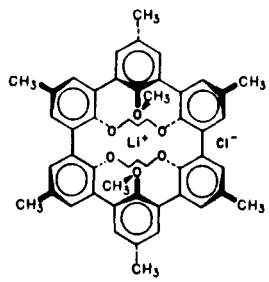

[B(A)(M$_3$)B]$_2$·LiCl (**4**·LiCl)

On the basis of CPK model examination, we had anticipated getting the anti isomers of [B(A)(M$_3$)B]$_2$ (*anti*-**4**) and [B(A)(EOE)B]$_2$ (*anti*-**5**).[8] These anti isomers in models can be easily assembled, and they appear only slightly more strained than models of A(AA)$_2$A (**1**). Molecular models of the *syn*-**4** and *syn*-**5** which were obtained cannot be assembled without shaving about 15% from the sides of the four bridge-terminating oxygens. The resulting models appear much more strained, and the cavities are less spherical than those of the anti isomers. Models also indicate there are no possible isomerizations of the syn and anti forms of the two bridged spherands without bonds being broken and made. This conclusion is confirmed by our preparation and characterization of (±)-**23** and both (±)-**24** and *meso*-**24**. These compounds are much less constrained than **4** and **5**, and yet they did not isomerize.[17b]

Molecular mechanical calculations on *anti*-[B(A)(M$_3$)B]$_2$·Li$^+$ (*anti*-**4**·Li$^+$) confirm it to be much more stable than its syn isomer.[18] We conclude either that for unexplained reasons *anti*-[B(A)(M$_3$)B]$_2$ (*anti*-**4**) or *anti*-[B(A)(EOE)B]$_2$ (*anti*-**5**) never formed or, more likely, they were formed in very small amounts but we were unsuccessful in isolating the compounds.

Encapsulation–Deencapsulation Reactions. When heated to 200 °C in water–pyridine, A(AA)$_2$A·LiCl (**1**·LiCl) demethylated to give the lithium salt, A(AA)A$^-$Li$^+$ (**22**), which when heated to 100 °C in aqueous HCl readily protonated to provide the free

(18) Kollman, P.; Wipff, G.; Singh, U. C. *J. Am. Chem. Soc.*, in press.

Chart IV

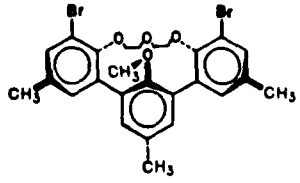

BrB(A)(EOE)BBr (21)

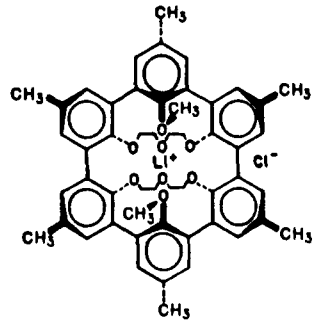

[B(A)(EOE)B]$_2$·LiCl (5·LiCl)

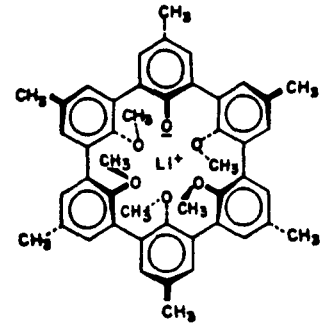

A(AA)$_2$A$^-$Li$^+$ (22)

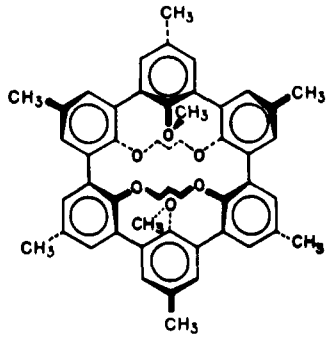

anti-4

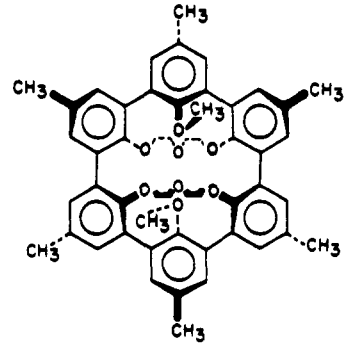

anti-5

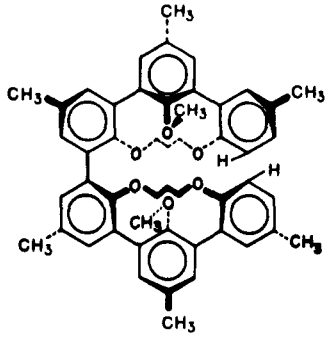

(±)-23

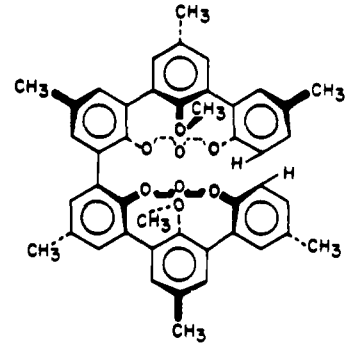

(±)-24

monophenol, A(AA)$_2$Ah (**6**, 70% overall). This demethylation is undoubtedly an SN_2 reaction in which Li^+ acts as an electrophile and Cl^- or pyridine as a nucleophile. When A(AA)$_2$Ah was treated with NaOH and Me_2SO_4, A(AA)$_2$A$^-$Na$^+$ was first generated and then methylated to give A(AA)$_2$A·NaCl (**1**·NaCl). Attempts to encapsulate K^+ by treatment of A(AA)$_2$Ah (**6**) with KOH and $(Me)_2SO_4$ produced only a mixture of free A(AA)$_2$A (**1**) and complex A(AA)$_2$A·NaCl (**1**·NaCl) in which Na^+ impurities had been scavenged from bulk KOH. Similar attempts to encapsulate Mg^{2+} and Ca^{2+} also failed, resulting in mixtures of Na^+-scavenged products and mixtures of phenoxide salts. Thus by the criteria of the outcome of these encapsulation reactions, A(AA)$_2$A (**1**) appears unique in its ability to complex only Li^+ and Na^+ and to exclude K^+, Mg^{2+}, and Ca^{2+}.

Crystal Structures. The single-crystal structures of A(AA)$_2$A (**1**), of its LiCl complex (**1**·LiCl), and of $NaSO_4CH_3$ complex (**1**·$NaSO_4CH_3$) were determined from diffraction photographs taken at 295 K. Complex **1**·$NaSO_4CH_3$ was prepared by methylating A(AA)$_2$A$^-$Na$^+$ with $(CH_3)_2SO_4$, which accounts for the $SO_4CH_3^-$ anionic component. The resulting structures were refined to give *R* values of 0.053, 0.047, and 0.15, respectively.[2b] The three structures are essentially identical with one another in their conformations and general shapes, whose plane projections resemble those of snowflakes. The notable difference between the three crystal structures is the *presence of an enforced cavity* in that of A(AA)$_2$A (**1**), which is filled with Li^+ in **1**·LiCl and with Na^+ in **1**·$NaSO_4CH_3$. Thus unlike the chorands and cryptands, Li^+ and Na^+ ions do not *have to conformationally re-*

organize their hosts when complexing spherand A(AA)$_2$A (**1**). The cavity, its lining of 24 electrons, the inner shell of six ether oxygens, and its outer shell of hydrocarbon support structure were all organized for binding during synthesis rather than during the complexing act. We suggest the term "preorganized" to describe such hosts.

Table I records values of selected distances and angles of interest in these three crystal structures. Those of **1** and **1**·LiCl possess D_{3d} symmetry, whereas **1**·$NaSO_4CH_3$ has lower symmetry, although the **1**·Na^+ cation within the crystal has approximately D_{3d} symmetry. There is some disorder of the $CH_3SO_4^-$ ion, and a molecule of solvent in the crystal structure of **3**·$NaSO_4CH_3$ complicated its refinement.[19] The structures of **1** and **1**·LiCl are very similar, with a slight lengthening along the C_3 axis in **1**·LiCl compared to **1**. The Li^+ in **1**·LiCl fills the octahedral cavity defined by its six oxygens. The Cl^- occupies a cavity defined in the crystal by 12 hydrocarbon groups. Three methoxymethyls are above the Cl^-, three are below, and six arylmethyls surround Cl^- in a median plane. Each Li^+ has two Cl^- neighbors at 5.2 Å along the C_3 axis and six more at 10.7 Å in adjacent parallel stacks of complexes. Drawing **25** represents superimposed cross sections of seven parallel stacks of spherand complexes viewed along the C_3 molecular axes. The three heavy circles represent

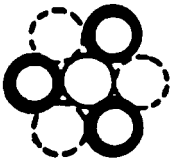

25

cross sections above the plane, the ordinary central circle is in the plane, and the three dashed circles are below the plane of the page. In the center of each circle is a Li^+, and above and below each circle is a Cl^-. Chart V provides drawings of the crystal structures of A(AA)$_2$A (**1**) and its two complexes.

The structural parameters of Table I provide evidence that A(AA)$_2$A (**1**), **1**·Li^+, and **1**·Na^+ contain different amounts of strain and provide clues as to the causes. (1) The six aryl groups in each of the three species are folded to different extents about their O–C_6H_4–CH_3 axes, the angles of fold being 6.3° for **1**, 4.8° for **1**·Na^+, and 2.6° for **1**·Li^+. (2) The distance the six oxygens of each species are bent out of the best planes of their attached aryls is 0.20 Å for **1**, 0.12 Å for **1**·Na^+, and 0.07 Å for **1**·Li^+. (3) The distance the twelve aryl carbons attached to aryls are bent out of the best planes of their reference aryls is 0.16 Å for all three species. By criteria 1 and 2, **1** > **1**·Na^+ > **1**·Li^+ in strain associated with nonplanarity of the aryl groups and their attached atoms.

A comparison of the hole diameters and the pseudoortho O·to·O distances provides a clue as to the origins of the strain. The hole diameter in free host **1** is 1.62 Å, larger than that of **1**·Li^+ (1.48 Å) but smaller than that of **1**·Na^+ (1.75 Å). The pseudoortho O·to·O distances in free host **1** are 2.92 Å, greater than the normal 2.80 Å van der Waal crystallographic distance. This increase probably reflects greater than usual O-to-O repulsions because of the enforced convergent orientations of the orbitals containing the twelve electron pairs of the six oxygens. These orbitals either contact one another or protrude into the vacuum of the hole. The dielectric properties of the micromedium of the C–O bond moments are between that of the vacuum of the hole on one side and the hydrocarbon shell on the other. When the vacuum is filled with Li^+ as in **1**·Li^+, the dielectric properties change, the pseudoortho O-to-O distance decreases to 2.78 Å (essentially normal van der Waals distance), and some strain is relieved. When the vacuum is filled with Na^+ as in **1**·Na^+, somewhat less strain is relieved, and the larger size of the Na^+ ion is accommodated by an increase in the six dihedral angles of the Ar–Ar linkages. We conclude that some of the driving force for complexation of **1** is the relief of bond angle strain of the host.

(19) Full details on these crystal structures will be published elsewhere.

Chart V. Crystal Structures of Spherands

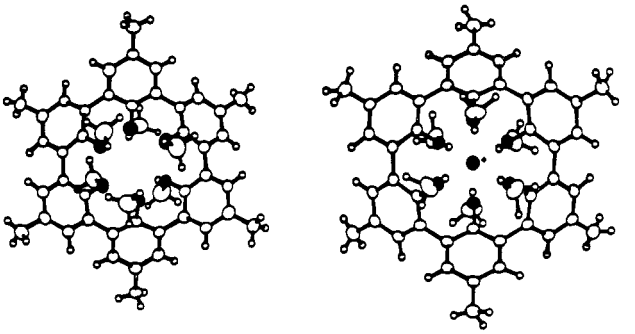

A(AA)$_2$A, **1** A(AA)$_2$A·Li^+ (**1**·Li^+) and A(AA)$_2$A·Na^+ (**1**·Na^+)

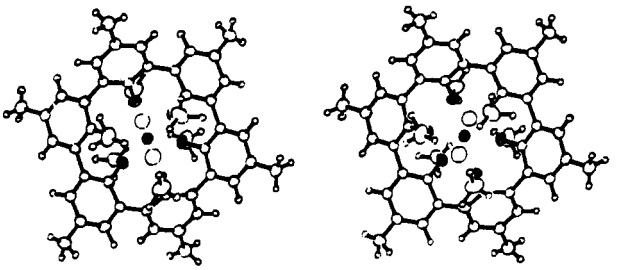

Stereodrawing of A(AA)$_2$A·ClLiCl$^-$ (**1**·ClLiCl$^-$)

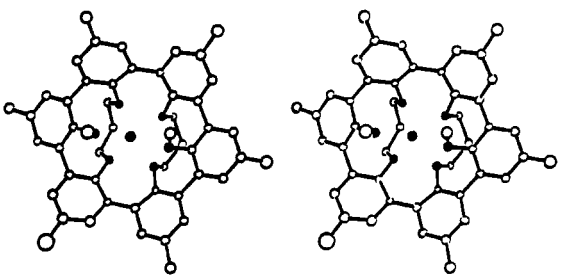

Stereodrawing of [B(A)(M_3)B]$_2$·Li^+ (**4**·Li^+)

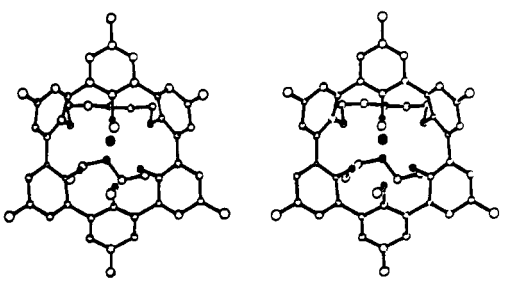

Stereodrawing of [B(A)(EOE)B]$_2$·Li^+ (**5**·Li^+)

The single-crystal structures of [B(A)(M_3)B]$_2$·$LiFeCl_4$ (**4**·$LiFeCl_4$) and of [B(A)(EOE)B]$_2$·LiCl (**5**·LiCl) were determined from diffraction photographs taken at 115 K. The structures were refined to R values of 0.064 and 0.070, respectively. Scheme I contains stereodrawings of the structures of **4**·Li^+ and **5**·Li^+. The structures of **4**·Li^+ and **5**·Li^+ in their crystals almost contain mirror planes bisecting their lithiums and CH_3O oxygens. The effect

Table II. Structural Parameters in Crystal Structures of $A(AA)_2A\cdot LiCl$ (**1**·LiCl), $[B(A)(M_3)B]_2\cdot LiFeCl_4$ (**4**·$LiFeCl_4$), and $[B(A)(EOE)B]_2\cdot LiCl$ (**5**·LiCl)

structural parameters		1·LiCl	4·$LiFeCl_4$	5·LiCl
no. of ligating O's		6	5	7
character nonligating O		none	OCH_3	OCH_3
	Distances (Å)			
Li diameters		1.48	1.27[a]	1.71[b]
Li to O	ligating, av	2.14	2.035	2.253
	ligating, range	0	2.00-2.09	2.03-2.42
	nonligating	none	2.88	3.48
close O to O	av	2.78	2.64[c]	2.67[d]
	range	none	2.50-2.73[c]	2.57-2.79[d]
O to best plane of attached aryl[e]	av	0.07	0.20	0.25
	range	none	0.08-0.33	0.04-0.39
C of attached aryls to best plane ref aryl[f]	av	0.16	0.29	0.33
	range	none	0.01-0.43	0.10-0.55
	Angles (deg)			
aryl folds on CH_3-Ar-O axis	av	2.6	8	8
	range	none	4-10	2-13
best planes Ar-Ar dihedral angle	av	56	43	45
	range	none	28-51	22-55

[a] Based on five O ligands. [b] Based on seven O ligands. [c] All six pseudoortho and one pseudometa O-to-O distances are included. [d] Four pseudoortho and four near O-to-O distances in $OCH_2CH_2OCH_2CH_2O$ bridges are included. [e] O's are bent out of best planes of their attached aryls. [f] C's of attached aryl are bent out of best planes of their reference aryls.

of the bridges in each of the two structures is essentially to "squeeze out" of ligating range *one* of the methoxyl oxygens to provide long lithium-to-oxygen distances of 2.88 and 3.48 Å in **4**·Li^+ and **5**·Li^+, respectively. The remaining five oxygens of **4**·Li^+ and seven oxygens of **5**·Li^+ ligate the Li^+ ions. Table II records the interesting structural parameters associated with **1**·Li^+, **4**·Li^+, and **5**·Li^+.[19]

The average Li^+ diameters were calculated by averaging the short Li^+-to-O distances and subtracting the radius of oxygen (1.40 Å).[20] The diameter varies with the number of ligating oxygens: with five oxygens, the diameter is 1.27 Å, with six oxygens, 1.48 Å, and with seven oxygens, 1.71 Å. The method is based on the assumptions that the Li^+ ion fills the whole volume and that the oxygens are not deformed from their normal diameters by their interpenetration of each other's diameters. Since the oxygens are preorganized rather than organized by the guest in these complexes, it is interesting to compare these diameters with those in which the guest organizes the ligating atoms. Average Li^+ diameters calculated from crystal structures of other selected compounds are as follows: four coordinate, tetrahedral, 1.12 Å; five coordinate, 1.36 Å; six coordinate, octahedral, 1.50 Å.[21] To our knowledge, no crystal structure of a seven-coordinate lithium complex has been reported previously.

The hosts of **4**·Li^+ and **5**·Li^+ are severely strained. All six of the pseudoortho and one of the pseudometa O-to-O distances in **4**·Li^+ are less than the normal van der Waals distance of 2.80 Å (average 2.64 Å, range 2.50–2.73 Å). In **5**·Li^+, the two bridge-terminating, pseudoortho O-to-O distances, the two shortest of the four CH_3O to pseudoortho $ArOCH_2$, and the four near O-to-O distances in the two OEOEO bridges average 2.67 Å, the range being 2.57–2.79 Å. Thus **4**·Li^+ contains seven and **5**·Li^+ eight shorter than usual O-to-O distances. In contrast, all of the pseudoortho O-to-O distances in **1**·Li^+ are close to being normal (2.78 Å). It is hardly surprising that CPK molecular models of **4**·Li^+ and **5**·Li^+ based on normal crystal structure diameters could not be assembled without shaving substantial amounts of material from their four bridge-terminating oxygens.

The benzene rings and their attached oxygen and aryl carbons in **4**·Li^+ and **5**·Li^+ are more displaced from their normal coplanar arrangement than in **1**·Li^+. The average angle of fold of the benzene rings around the CH_3–Ar–O axis is only 2.6° in **1**·Li^+, but it is 8° in **4**·Li^+ and **5**·Li^+ (as high as 13° in one benzene). The average distance the six oxygens are bent out of the best planes of their attached benzenes is only 0.07 Å in **1**·Li^+ compared to 0.29 Å in **4**·Li^+ and 0.33 Å in **5**·Li^+. The average distance the twelve aryl carbons are bent out of the best planes of their attached reference benzene rings is only 0.16 Å in **1**·Li^+ compared to 0.20 Å in **4**·Li^+ and 0.33 Å in **5**·Li^+. The average dihedral angle about the best planes Ar–Ar bond in **1**·Li^+ is 56°, but it is decreased to 43° in **4**·Li^+ (range 28–51°) and to 45° (range 22–55°) in **5**·Li^+. We were unsuccessful in obtaining suitable crystals for X-ray analysis of free hosts **4** and **5**. However, their CPK molecular models (four O's shaved) indicate them to be much more rigid than those of either **1** or *anti*-**4** or *anti*-**5**. Therefore the free hosts **4** and **5** are at least as likely to resemble their Li^+ complexes as free host **1** resembles its Li^+ complex.

Using the CPK molecular models to design and construct **1**, **1**·Li^+, and **1**·Na^+ and the shaved CPK models to construct **4**·Li^+ and **5**·Li^+ led to structures greatly resembling those observed in their crystal structures. For example, the D_{3d} symmetry of the up–down–up–down–up–down arrangement of the OCH_3 groups in **1** and its complexes are predicted in advance of experiment. The five close and one far Li^+-to-O distances in *syn*-**4**·Li^+ are visible in models as are the seven close and one far Li^+-to-O distances in *syn*-**5**·Li^+. Models of the two latter complexes differ little from those of the free spherands or from those of their Na^+ complexes. Although models of **1**·K^+ can be constructed, the orbitals of the unshared electron pairs on the oxygens do not converge on the potassium ion because of its large size. Instead of contacting these orbitals, K^+ contacts the middle of the polarized C–O bonds, which electrostatically should be nonideal for binding. Models of *syn*-**4**·K^+ cannot be constructed at all, and those of *syn*-**4**·K^+ suffer the same defect as those of **1**·K^+. Thus CPK molecular models are very useful both in designing complementary and preorganized host–guest relationships and in predicting the patterns of near and far binding sites in the rigid systems **4** and **5**.

The CPK models broke down completely in predicting the up–down–down–up–down–down arrangement of the oxygens in **4** and **5**. Before the crystal structure determinations of their Li^+ complexes, **4** and **5** were assigned the up–down–up–down–up–down structures (*anti*-**4** and *anti*-**5**) that can be made with unshaved CPK molecular models.[8] In predicting structures of complexes assembled from their individually stable host and guest components, CPK models serve well because binding energies are insufficient to deform bonds greatly and compress atoms. However, the final ring-closing step in the syntheses of **4** and **5** involved what probably is a lithium ion-templated coupling of two aryl radicals with the release of enough energy to pay high molecular deformation costs. Host (±)-**23** resembles *anti*-**4** and *meso*-**23** resembles *syn*-**4**, the two sets of compounds differing only in the sense that in the isomers of **23**, two C–H bonds replace a C–C bond of **4**. Host (±)-**24** and *anti*-**5**, and *meso*-**24** and *syn*-**5** possess similar relationships. The fact that the (±)-**23** and (±)-**24** isomers dominated in their syntheses and that the *syn*-**4** and *syn*-**5** isomers dominated in their syntheses remains a mystery that invites further study.

Spectral Properties. Table III records the chemical shifts and the assignments of the protons in the ^1H NMR spectra of **1**–**6** and of $A(AA)_2A\cdot Li^+$ (**22**). The patterns of the numbers of different kinds of protons indicate that the symmetry properties of the hosts in solution are the equivalent of those in the crystal structures for those systems where data are available. Furthermore, the free and complexed spherands where examined show the same patterns, which indicates the hosts are not conformationally reorganized during complexation in any other than minor ways. Thus $A(AA)_2A$ (**1**), **1**·LiCl, **1**·LiBr, **1**·$LiClO_4$, **1**·NaCl, and **1**·NaBr all provide three singlets consistent with the D_{3d} symmetry of **1**, **1**·Li^+, and **1**·Na^+ in their crystal structure. The changes in chemical shifts of these singlets as **1** is complexed with different guests varies between a minimum of 0.02 ppm and a maximum

(20) Pauling, L. C. "The Nature of the Chemical Bond"; 3rd ed.; Cornell University Press; Ithaca, NY, 1960; p 260.
(21) Hermansson, K.; Thomas, J. O.; Olovsson, I. *Acta. Crystallogr., Sect. B* **1977**, *B53*, 2859–2861.

Table III. Chemical Shifts (δ) in ^{1}H NMR Spectra (200 MHz, $CDCl_3$)[a]

compound	Ar–CH_3	O–CH_3	Ar–H	bridges or OH
A(AA)$_2$A (**1**)	2.41 (s, 18 H)	2.85 (s, 18 H)	7.17 (s, 12 H)	
1·LiCl	2.50 (s, 18 H)	3.09 (s, 18 H)	7.33 (s, 12 H)	
1·LiBr[b]	2.50 (s, 18 H)	3.09 (s, 18 H)	7.33 (s, 12 H)	
1·$LiClO_4$	2.50 (s, 18 H)	3.06 (s, 18 H)	7.34 (s, 12 H)	
1·NaCl	2.48 (s, 18 H)	3.01 (s, 18 H)	7.31 (s, 12 H)	
1·NaBr[b]	2.48 (s, 18 H)	3.02 (s, 18 H)	7.31 (s, 12 H)	
A(AA)$_2$P (**2**)	2.38 (s, 6 H)	2.72 (s, 6 H)	7.11–7.50 (m, 13 H)	
	2.40 (s, 3 H)	2.98 (s, 3 H)		
	2.44 (s, 6 H)	3.12 (s, 6 H)	8.50 (br s, 1 H)	
2·$LiClO_4$	2.49 (s, 6 H)	3.04 (s, 6 H)	7.09 (br s, 1 H)	
	2.51 (s, 3 H)	3.13 (s, 6 H)	7.32–7.72 (m, 13 H)	
	2.53 (s, 6 H)	3.19 (s, 3 H)		
2·$NaClO_4$	2.47 (s, 6 H)	2.95 (s, 6 H)	6.79 (br s, 1 H)	
	2.48 (s, 3 H)	3.04 (s, 9 H)	7.30–7.72 (m, 13 H)	
	2.50 (s, 6 H)			
P(AA)$_2$P (**3**)	2.42 (s, 12 H)	3.00 (s, 12 H)	7.18–7.51 (m, 14 H), 8.58 (br s, 2 H)	
[B(A)(M$_3$)B]$_2$ (**4**)	2.41 (s, 12 H)	2.80 (s, 6 H)	7.21 (s, 4 H), 7.24	0.45–0.65 (m, 2 H), 1.6–1.8 (m, 2 H),
	2.44 (s, 6 H)		(s, 4 H), 7.60 (s, 4 H)	3.15–3.35 (m, 4 H), 4.26 (br t, 4 H)
4·LiCl	2.49 (s, 12 H)	2.89 (s, 6 H)	7.35 (s, 4 H), 7.40	0.85–1.05 (m, 2 H), 1.9–2.1 (m, 2 H),
	2.51 (s, 6 H)		(s, 4 H), 7.79 (s, 4 H)	3.25–3.45 (m, 4 H), 4.48 (br t, 4 H)
4·LiBr[b]	2.49 (s, 12 H)	2.89 (s, 6 H)	7.34 (s, 4 H), 7.40	0.84–1.08 (m, 2 H), 1.93–2.18 (m, 2 H),
	2.52 (s, 6 H)		(s, 4 H), 7.78 (s, 4 H)	3.28–3.48 (m, 4 H), 4.43–4.62 (m, 4 H)
4·NaCl[b]	2.49 (s, 12 H)	2.92 (s, 6 H)	7.35 (s, 4 H), 7.40	0.61–0.92 (m, 2 H), 1.74–1.98 (m, 2 H),
	2.51 (s, 6 H)		(s, 4 H), 7.83 (s, 4 H)	3.18–3.43 (m, 4 H), 4.19–4.42 (m, 4 H)
4·NaBr[b]	2.51 (s, 6 H)	2.90 (s, 6 H)	7.35 (s, 4 H), 7.40	0.67–0.89 (m, 2 H), 1.78–2.0 (m, 2 H),
	2.49 (s, 12 H)		(s, 4 H), 7.83 (s, 4 H)	3.24–3.44 (m, 4 H), 4.27–4.45 (m, 4 H)
[B(A)(EOE)8]$_2$ (**5**)	2.35 (s, 12 H)	2.29 (s, 6 H)	7.03 (s, 4 H), 7.27	2.9–3.1 (m, 4 H), 3.6–3.4 (m, 4 H),
	2.47 (s, 6 H)		(s, 4 H), 7.34 (s, 4 H)	3.8–4.0 (m, 4 H), 4.2–4.4 (m, 4 H)
5·LiCl	2.39 (s, 12 H)	2.28 (s, 6 H)	7.05 (s, 4 H), 7.38	3.0–3.15 (m, 4 H), 3.8–4.0 (m, 8 H),
	2.52 (s, 6 H)		(s, 4 H, 7.55 (s, 4 H)	4.1–4.25 (m, 4 H)
5·LiBr[b]	2.39 (s, 12 H)	2.28 (s, 6 H)	7.05 (s, 4 H), 7.38	3.0–3.17 (m, 4 H), 3.77–4.03 (m, 8 H),
	2.53 (s, 6 H)		(s, 4 H), 7.56 (s, 4 H)	4.11–4.32 (m, 4 H)
5·NaCl[b]	2.40 (s, 12 H)	2.28 (s, 6 H)	7.05 (s, 4 H), 7.40	2.9–3.14 (m, 4 H), 3.71–3.97 (m, 8 H),
	2.53 (s, 6 H)		(s, 4 H), 7.65 (s, 4 H)	4.23–4.40 (m, 4 H)
5·NaBr[b]	2.40 (s, 12 H)	2.29 (s, 6 H)	7.05 (s, 4 H), 7.40	3.0–3.14 (m, 4 H), 3.74–3.99 (m, 8 H),
	2.53 (s, 6 H)		(s, 4 H), 7.65 (s, 4 H)	4.23–4.42 (m, 4 H)
A(AA)$_2$Ah (**6**)	2.40 (s, 9 H)	2.75 (s, 6 H)	7.14–7.25 (m, 12 H)	6.55 (s, 1 H, OH)
	2.45 (bs, 9 H)	2.96 (s, 3 H)		
A(AA)$_2$A$^-$Li$^+$ (**24**)	2.32 (s, 3 H)	2.99 (s, 9 H)	7.05–7.35 (m, 10 H)	
	2.40 (s, 6 H)	3.16 (s, 6 H)		
	2.46 (s, 3 H)			
	2.47 (s, 6 H)			

[a] Concentrations, 0.0014 to 0.0028 M. [b] $CDCl_3$ saturated with D_2O as solvent.

of 0.24 ppm. As expected from molecular model examination, the dihedral angle between the ArOCH$_3$ and best aryl planes can vary differently depending on the absence or presence of guests of differing size. This angle varies from 62° to 85° to 84° in passing from the crystal structure of **1** to that of **1**·Li$^+$ to that of **1**·Na$^+$ (Table I). The CH$_3$O proton moves from 2.85 to 3.09 to 3.01 ppm in the ^{1}H NMR spectrum in passing from **1** to **1**·Li$^+$ to **1**·Na$^+$. To a small extent the methyl hydrogens can move relative to the shielding cones of the pseudoortho phenyls. They appear to be more shielded in the free host than in the complexes. This effect is interpreted as reflecting the small realignment of dipoles that occurs when a cation fills what was previously a vacuum.

The patterns of chemical shifts of the Ar–CH_3, *O*CH_3, and Ar–H protons in the ^{1}H NMR spectra of [B(A)(M$_3$)B]$_2$ (**4**), **4**·Li$^+$, [B(A)(EOE)B]$_2$ (**5**), and **5**·Li$^+$ are consistent with their possessing C_{2v} symmetry or its equivalent in solution. However, the crystal structures of **4**·Li$^+$ and **5**·Li$^+$ essentially possess C_s symmetry, with one distant Ar–O–CH$_3$ in each complex at the end of an elongated cavity. In solution, it appears that the Li$^+$ moves rapidly on the ^{1}H NMR time scale back and forth in the elongated cavity, making the CH$_3$–Ar–OCH$_3$ groups at the termini the equivalent of one another. Equivalent reorganizations are observable in molecular models of both the free hosts and complexes. The changes in chemical shifts of the Ar–CH_3, OCH_3, and Ar–H singlets in passing from the free ligands to their Li$^+$ complexes range from 0.02 to 0.21 ppm, values compatible with minor reorganizations required for complexation. The M$_3$ and EOE bridges in models are more conformationally mobile, and larger chemical shift changes are observed upon complexation. For example, two protons in the CH$_2$CH$_2$CH$_2$ bridge of **4** and **4**·Li$^+$ are highly shielded, occurring as multiplets at 0.45–0.65° in **4** and at 0.85–1.05° in **4**·Li$^+$. Similar changes and conclusions apply to **4** vs. **4**·Na$^+$. Model examination indicates that the compression of the ring system forces two to four protons strongly into the shielding cone of the CH$_3$ArOCH$_3$ aryl groups. The extent of this compression appears to vary from the free host to the complexes, and it probably involves minor conformational reorganizations in the CH$_2$CH$_2$CH$_2$ bridge that accompany complexation. Similar changes are observed for **5**, **5**·Li$^+$, and **5**·Na$^+$. Although conformationally mobile in a very limited sense, the CH$_2$ groups in the bridges of **4** and **5** are much too large to turn inward and fill the cavities.

The patterns of chemical shifts of the Ar–CH_3, OCH_3, and Ar–H singlets in the spectra of A(AA)$_2$P (**2**), A(AA)$_2$Ah (**6**), and A(AA)$_2$A$^-$Li$^+$ (**24**) are consistent with the compounds possessing C_s symmetry, with a down–up–down–up–down arrangement of OCH$_3$ methyl groups in passing around the macroring from 2 o'clock to 10 o'clock in their drawings. The values of the chemical shifts are close to those of A(AA)$_2$A (**1**) and its complexes and suggest that all OCH$_3$ methyl groups are oriented outward away from the cavity. Although CPK molecular models of A(AA)$_2$P (**2**) and even A(AA)$_2$Ah (**6**) can be constructed with one or two methyl groups turned inward, the bond angle strain and compression introduced in such conformations make them unlikely. The compression in such conformations appears in models to be similar to that observed in like conformations of A(AA)$_2$A itself. The chemical shifts of the OCH$_3$ methyls in **2**, **6**, and **24** vary only

between δ 2.72 and 3.16, whereas those of $A(AA)_2A$ and its complexes vary from δ 2.85 to 3.09.

The Ar–H hydrogen which helps to line the cavity (it replaces the OCH_3 group of $A(AA)_2A$) provides a chemical shift which changes from δ 8.50 in $A(AA)_2P$ (**2**) to δ 7.09 in **2**·Li^+ to δ 6.79 in **2**·Na^+. This large change is attributed to the changes in positions of this proton relative to the shielding vs. the deshielding region of the two flanking aryls. The relevant aryl–aryl dihedral angles must change markedly in passing from **2** to **2**·Li^+ to **2**·Na^+.

Unlike models of **1**, **2**, and **4**–**6**, those of $P(AA)_2P$ (**3**) suggest that methoxyl groups can ring invert at ordinary temperatures. Thus it is not surprising that the CH_3O methyl protons occur as a singlet in the ^1H NMR spectrum of the compound at 30 °C. Molecular models suggest that the least compressed conformation for **3** possesses C_{2h} symmetry as drawn. In this conformation, the oxygens possess a square-planar arrangement, and all CH_3O groups are in equivalent magnetic environments. A much less probable alternative and more compressed C_2 conformation (molecular models) provides a larger cavity with the oxygens in a roughly tetrahedral arrangement. The chemical shift of the two Ar–H hydrogens facing the cavity (they take the place of two methoxyls of $A(AA)_2A$ that are pseudopara to one another) are found at δ 8.58, close to the value of δ 8.50 observed for the similar Ar–H hydrogen in $A(AA)_2P$ (**2**). Since the organization of $A(AA)_2A$ (**1**) is clear, and since the ^1H NMR patterns of **1** and **2** and their complexes resemble each other, the conformation of **2** must resemble that of **1**. The same organization appears likely for $P(AA)_2P$ (**3**) as well.

Appropriate mixing experiments of the spherand hosts and their complexes demonstrated that cation exchanges were slow on the ^1H NMR time scale at 30 °C. As expected, a mixture of $A(AA)_2A$·LiCl and $A(AA)_2A$·$LiClO_4$ gave averaged chemical shifts whereas a mixture of $A(AA)_2A$·LiCl and $A(AA)_2A$·NaCl gave additive spectra. Mixtures of $A(AA)_2A$·LiCl and $A(AA)_2A$, of $A(AA)_2A$·NaCl and $A(AA)_2A$, of $[B(A)(M_3)B]_2$·LiCl and $[B(A)(M_3)B]_2$, and of $[B(A)(EOE)B]_2$·LiCl and $[B(A)(EOE)B]_2$ gave additive rather than averaged spectra at 25 °C.

The ultraviolet absorption spectra in ethanol of several complexes were examined. The values for λ_{max} (nm) are as follows: $A(AA)_2A$·LiCl, 237 and 282; $A(AA)_2A$·NaCl, 228 and 278; $[B(A)(M_3)B]_2$·LiCl, 254 and 328 (shoulder); $[B(A)(EOE)B]_2$·LiCl, 251 and 322 (shoulder). These marked differences between the complexes are probably associated with the differences in the departure of the benzene rings and their attached atoms from their normal planar geometry coupled with the deformations of the aryl oxygen orbitals associated with their compression.[22] The latter effect would apply mainly to the bridged complexes, whose bridged aryl oxygens violate each other's normal van der Waals radii (see Table II).

The mass spectra of $A(AA)_2A$ (**1**), $[B(A)(M_3)B]_2$ (**4**), and $[B(A)(EOE)B]_2$ (**5**) and their complexes were taken on an MS 9 spectrometer at 70 eV with an inlet temperature of 180 °C unless specified otherwise. The three free hosts gave strong molecular (parent) ion peaks at 720, 744, and 804 (230 °C, inlet), respectively. Free host **1** also gave a substantial peak corresponding to $A(AA)_2Ah$ at 706. Complex **1**·LiBr gave a peak corresponding to $A(AA)_2A^-Li^+$ at 712 and a substantial peak corresponding to $A(AA)_2Ah$ at 706, but no peak at 720 for free **1**; **1**·NaBr gave a substantial peak at 728 corresponding to $A(AA)_2A^-Na^+$, no peak at 720, and a strong peak at 706 corresponding to $A(AA)_2Ah$. Complex **4**·LiBr (inlet, 240 °C) gave a strong peak at 600 and none above this mass. Complex **4**·NaBr (inlet, 220 °C) gave a series of peaks of increasing intensities at 744 (free **4**), 730 (**4**-CH_2), 672 and 600. Complex **5**·LiBr (inlet, 230 °C) gave a substantial peak at 670 and a strong peak at 626. Complex **5**·NaBr (inlet, 210 °C) gave a small peak at 804 (free **5**), a substantial peak at 772, and a strong peak at 627. Thus, the complexes of **1** in the mass spectrometer demethylate to form host–guest salts, whereas those of **4** and **5** undergo other fragmentations.

Complexation Experiments. The differences in ^1H NMR of the free and complexes hosts were used to determine which ions were complexed by $A(AA)_2A$ (**1**), $A(AA)_2P$ (**2**), $P(AA)_2P$ (**3**), $[B(A)(M_3)B]_2$ (**4**), and $[B(A)(EOE)B]_2$ (**5**). Solutions (500 μL) of these hosts in $CDCl_3$ (~0.002 M) were mixed with 10 μL of $(CD_3)_2SO$ solutions that were ~0.04 M in $LiClO_4$·$3H_2O$, or $NaClO_4$·H_2O, $KClO_4$, $RbClO_4$, $CsClO_4$, $Mg(ClO_4)_2$, $Ca(ClO_4)_2$, or $La(ClO_4)_3$. In the resulting homogeneous solutions of potential binding partners, the molar ratios of host to guest were approximately 2.2 to 1. The ^1H NMR spectra (200 MHz) were taken at 35 °C within 5 min to 3 h of mixing. All solutions gave signals for the free hosts that were present, but only in the solutions containing $LiClO_4$ or $NaClO_4$ and $A(AA)_2A$ (**1**), $A(AA)_2P$ (**2**), $[B(A)(M_3)B]_2$ (**4**), and $[B(A)(EOE)B]_2$ (**5**) was there evidence of complex formation. The four spherands appear to complex Li^+ and Na^+ completely and immediately but to reject the other ions. Compound $P(AA)_2P$ (**3**) showed no evidence for complexing any of the ions.

We interpret the specificity of **1**, **2**, **4**, and **5** in terms of the principles of complementarity and preorganization. All four hosts are preorganized with cavity sizes close to the diameters of Li^+ and Na^+, but distant from the diameters of the other alkaline earth ions. The diameters of Mg^{2+}, Ca^{2+}, and La^{3+} are within the range of the cavity sizes of these spherands. However, molecular model examination indicates that during complexation, for steric reasons most of the ligands must be stripped from the guest before the ions can enter the lipophilic sleeves that lead to the cavity. In $A(AA)_2A$ (**1**), the lipophilic sleeve is composed of methyl groups. Unlike the flexible chorands or cryptands, the ligands of the host cannot displace the ligands of the guest one at a time until the complex is fully formed. The heats of ligation of the multiply charged ions are too high for them to reach a low enough ligation level to enter the lipophilic sleeves. Preliminary results of attempts to encapsulate Mg^{2+} by treating A(AA)Ah with CH_3MgBr followed by $(CH_3)_2SO_4$ resulted in loss of a second methyl group to form what is probably $A^-(AA)A^-$·Mg^{2+}. It is probable that if a way is found to get these multiply charged ions to enter the cavities of the spherands, these ions would be strong enough Lewis acids to cause easy loss of alkyl groups to produce zwitterionic complexes.

Extraction Experiments. In a series of extraction experiments, ~0.002 M solutions of hosts $A(AA)_2A$ (**1**), $[B(A)(M_3)B]_2$ (**4**), and $[B(A)(EOE)B]_2$ (**5**) in $CDCl_3$ were mechanically (violently) shaken with equal volumes of potential guest salts dissolved in D_2O. Potential guest salts of the highest purity purchasable were employed. Quartz-Teflon equipment was used. The progress of complexation was followed with ^1H NMR spectral measurements on the $CDCl_3$ phase or by mass spectral measurements on the solids recovered form that phase.

The results are as follows. (1) All three hosts (**1**, **4**, and **5**) became fully complexed when the D_2O phase was 6 M in NaBr, LiBr, or NaCl in a matter of 1–42 h. When the D_2O phase was 0.2 M NaCl, **1** was fully complexed in 76 h, **5** in 124 h, whereas **4** remained only 7% complexed from 20 to 198 h. When the D_2O phase was 0.2 M LiCl, **1** was fully complexed in 763 h, **4** was 93% complexed in 769 h (nonequilibrated), and **5** was 61% complexed in 669 h (nonequilibrated). (2) In a competition experiment, a mixture of 0.1 M NaCl and 0.1 M LiCl was extracted. With **1** as host, full complexation was reached after 277 h. Throughout the extraction, the ratio of % NaCl to LiCl complexed was about 7 to 1. (3) When shaken with 3–6 M solutions of KBr, $MgBr_2$, or $CaBr_2$, only *Na^+ impurities* were scavenged from the aqueous phases by all three hosts. The same was observed when **1** was used with CsCl and $SrBr_2$ and **4** with $SrBr_2$. (4) Attempts failed to complex HX by **1** through 168-h extractions of D_2O, 0.5 M in HBr, or 0.6 M in HCl. (5) Solutions of **1**·LiCl, **4**·LiCl, and **5**·LiCl (~0.0027 M) in $CDCl_3$ were shaken with equal volumes of D_2O. In 280 h, **1**·LiCl was 0% decomplexed, **4**·LiCl was 79% decomplexed (nonequilibrated), and **5**·LiCl was 63% decomplexed (nonequilibrated). Similar experiments were conducted with

(22) For an early example of the changes in UV spectra with departures of benzene rings from their normal planar geometries, see: Cram, D. J.; Montgomery, C. S.; Knox, G. R. *J. Am. Chem. Soc.* **1966**, *88*, 515–525.

1·NaCl, 4·NaCl, and 5·NaCl. In 402 h, 1·NaCl was 81% decomplexed (nonequilibrated); in 21 h, 4·NaCl was 100% decomplexed; in 221 h, 5·NaCl was 86% decomplexed (equilibrated).

These results suggest the following conclusions. Only Na^+ and Li^+ ions can be extracted from aqueous solutions by $CDCl_3$ solutions of hosts $A(AA)_2A$ (**1**), $[B(A)(M_3)B]_2$ (**4**), and $[B(A)(EOE)B]_2$ (**5**). Nonextracted ions are H^+, K^+, Cs^+, Mg^{2+}, Ca^{2+}, and Sr^{2+}. The extractions are slow because of the low solubilities of hosts in the aqueous phase and of the guests in the organic phase and because interfacial complexation is inhibited by the hydrocarbon skin of these preorganized hosts. Sodium salts are extracted faster than lithium salts by a factor of about 7 with **1** as host. This ratio did not change with time because of the fiftyfold excess of Na^+ (and Li^+) over **1** involved and because the decomplexation rates must have been too slow for $1{\cdot}Na^+$ to equilibrate with $1{\cdot}Li^+$. The order of the thermodynamic stabilities of the complexed spherands reported in other quantitative experiments is $1{\cdot}Li^+ \gg 1{\cdot}Na^+ \sim 5{\cdot}Na^+ > 4{\cdot}Li^+ \sim 5{\cdot}Li^+ > 4{\cdot}Na^+$.[9,23] The extraction experiments reported here are too fragmentary to confirm this order, but they are fully consistent with it.

Values of association constants (K_a) and free energies of binding ($-\Delta G°$) by $A(AA)_2P$ in $CDCl_3$ of lithium and sodium picrates dissolved in D_2O were determined by extraction experiments[13b,24] that lasted hours or days before equilibrium was reached. The $-\Delta G°$ value for $A(AA)_2P$ binding lithium picrate in $CDCl_3$ saturated with D_2O at 25 °C was 10.4 kcal mol^{-1}, and for $A(AA)_2P$ binding sodium picrate it was 6.6 kcal mol^{-1} under the same conditions. The ratio $K_a^{Li}/K_a^{Na} = 630$ provides a measure of the structural recognition which this host shows for lithium as compared to sodium ion. The binding free energies were too high and the rates of equilibrium too low to allow this technique to be applied to the other spherands. Indirect methods to obtain K_a and $-\Delta G°$ values for the other spherands will be described in the companion paper in this series. The discussion of the values reported here are reserved for that paper.

Conclusions. These experiments provide the following general conclusions. (1) Through use of CPK models, host systems can be designed containing enforced cavities complementary to Li^+ and Na^+, both in an electronic and a steric sense. The crystal structures of the free ligand systems and their complexes coupled with their ^1H NMR spectra confirm that the systems undergo little conformational reorganization during complexation and are therefore preorganized. The binding sites of these spherands are shielded by their support structures from solvation. (2) The enforced and preorganized structures of these hosts are responsible for their being very powerful and highly discriminating binders of Na^+ and Li^+ ions. Anisole and similar compounds are generally poor and nondiscriminating ligating species. (3) The power of the principles of complementarity and preorganization is illustrated by the invention of the spherands.

Experimental Section

3,3″-Dibromo-5,5′,5″-trimethyl[1,1′:3′,1″-terphenyl]-2,2′,2″-triol (BrAhAhAhBr), Procedure A. To a stirred solution of HAhAhAhH (**9**) (20.0 g or 62.5 mmol) in $CHCl_3$ (60 mL) was added dropwise (1 h at 25 °C) a solution of 26.0 g (0.163 mol) of Br_2 in $CHCl_3$ (200 mL). The mixture was stirred for 0.5 h, washed with a dilute aqueous solution of Na_2SO_3 and water, and dried. The solvent was evaporated under reduced pressure to give 29.7 g (~100%) of crude BrAhAhAhBr, mp 269–273 °C dec. For analysis a small sample was recrystallized from EtOH, mp 273–275 °C (dec); MS, M^+ 476 (^{79}Br). Anal. ($C_{21}H_{18}Br_2O_3$) C, H.

3,3″-Dibromo-2,2′,2″-trimethoxy-5,5′,5″-trimethyl[1,1′:3′,1″-terphenyl], or BrAAABr (11), Procedure B. To a stirred mixture of 44 g (0.67 mol) of 85% KOH in H_2O and of 30.0 g (62.8 mmol) of BrAhAhAhBr in 330 mL of THF was added 38 g (0.30 mol) of $(CH_3)_2SO_4$ dropwise over a 10-min period. The mixture was stirred at reflux temperature for 1 h, and the THF was evaporated under reduced pressure. The residue was extracted with ether from water and after the usual isolation procedure (washing, drying, evaporating) gave a yellow viscous oil (35 g). This material was passed through 90 g of Al_2O_3 (Woelm, neutral activity I) with pentane–benzene (10:1) as the mobile phase to give 28.1 g (86%) of **11** as a colorless gum. For analysis a small sample was purified by preparative TLC; MS, M^+ 518 (^{79}Br). Anal. ($C_{24}H_{24}Br_2O_3$) C, H.

5,5′,5″,5‴,5⁗,5⁗′-Hexamethyl[1,1′:3′,1″:3″,1‴:3‴,1⁗:3⁗,1⁗′:3⁗′,1⁗′′-sexiphenyl]-2,2′,2″,2‴,2⁗,2⁗′-hexaol (17). A solution of 31.0 g (0.0969 mol) of crude HAhAhAhH (**9**) in 434 mL of CH_3CN–145 mL of H_2O was mixed with 262 g (0.969 mol) of powdered $FeCl_3{\cdot}6H_2O$, and the resulting mixture was magnetically stirred for 7 days at 25 °C. The crystalline powder that separated was collected, washed well with a mixture of 50 mL of CH_3CN–50 mL of H_2O–10 mL of concentrated H_3O^+, triturated with a like mixture, again collected and washed well with H_2O, and dried to give **17** as tan crystals (10.6 g). This material was dissolved in 200 mL of pyridine, 1 L of xylene was added, and the filtered mixture was evaporated at 30 mm of pressure until crystals appeared. The mixture was cooled to 25 °C, white product was collected, washed successively with C_6H_6 and hexane, and dried to give 5.3 g (17%) of **17**, mp 310–314 °C dec. An analytical sample was prepared by sublimation at 0.1 mm of pressure and about 300 °C, mp 310–314 °C dec; MS, M^+ 638. Anal. ($C_{42}H_{38}O_6$) C, H.

From the original filtrate was recovered 14.6 g (47%) of unreacted **9**. When the reaction period was extended to 15 days and the molar ratio of $FeCl_3{\cdot}6H_2O$ to **9** was increased to 20, a 47.5% yield of **17** was obtained. R_f value, precoated TLC plate (SiO_2 60F-254, E. Merck) 0.42 ((THF), 0.57 (EtOAc)).

2,2′,2″,2‴,2⁗,2⁗′-Hexamethoxy-5,5′,5″,5‴,5⁗,5⁗′-hexamethyl[1,1′:3′,1″:3″,1‴:3‴,1⁗:3⁗,1⁗′:3⁗′,1⁗′′-sexiphenyl], H(A)$_6$H. Application of Procedure B to 10.0 g of $H(Ah)_6H$ gave product purified by passage in C_6H_6 through 40 g of SiO_2 to give 7.9 g (70%) of $H(A)_6H$. A small sample was fractionally (molecularly) distilled with a differential subliming apparatus at 300–350 °C at ~0.1 mm to give $H(A)_6H$ as a glass with transition temperature 115–130 °C: MS, M^+ 722; ^1H NMR ($CDCl_3$, 100 MHz) δ 2.31 (s, 6 H, $ArCH_3$), 2.34 (s, 12 H, $ArCH_3$), 3.26 (s, 6 H, CH_3O), 3.37 (s, 6 H, CH_3O), 3.75 (s, 6 H, OCH_3), 6.86 (d, J = 8.0 Hz, 2 H, ArH), 7.04–7.17 (m, 12 H, ArH). Anal. ($C_{48}H_{50}O_6$) C, H.

3,3⁗′-Dibromo-2,2′,2″,2‴,2⁗,2⁗′,2⁗′′-hexametoxy-5,5′,5″,5‴,5⁗,5⁗′-hexamethyl[1,1′:3′,1″:3″,1‴:3‴,1⁗:3⁗,1⁗′:3⁗′,1⁗′′-sexiphenyl] (19), Br(A)$_6$Br. Application of Procedure A to 11.9 g of crude $H(Ah)_6H$ gave 15.1 g (~100%) of crude $Br(Ah)_6Br$ (**18**), a small sample of which was recrystallized from degassed pyridine–xylene, mp 272–280 °C dec. Without further characterization, the total amount of **18** was methylated by procedure B to give 16.2 g of crude $Br(A)_6Br$. This material was chromatographed on 500 g of SiO_2 with hexane–EtOAc (11:3) as the mobile phase to give $Br(A)_6Br$ (**19**), 8.4 g (50%, overall), as a white foam. For analysis, a small sample was fractionally (molecularly) distilled with a differential subliming apparatus at 300–350 °C (0.1 mm) to give material with a glass transition temperature of 123–124 °C: MS, M^+ 878 (^{79}Br); ^1H NMR ($CDCl_3$, 100 MHz) δ 2.30 (s, 6 H, $ArCH_3$), 2.34 (s, 12 H, $ArCH_3$), 3.29 (s, 6 H, OCH_3), 3.33 (s, 6H, OCH_3), 3.55 (s, 6 H, OCH_3), 7.10 (br s, 4 H, ArH), 7.17 (br s, 6 H, ArH), 7.36 (br s, 2 H, ArH). Anal. ($C_{48}H_{48}O_6Br_2$) C, H, Br.

2′-Methoxy-5,5′,5″-trimethyl[1,1′:3′,1″-terphenyl]-2,2″-diol (15), HAhAAhH. A mixture of 50 g (0.156 mol) of HAhAhAhH (**9**), 23.7 g (0.172 mol) of K_2CO_3, 200 mL of reagent acetone, and 25 mL (0.40 mol) of CH_3I was stirred under N_2 in the dark at 25 °C for 26 h. The mixture was evaporated under reduced pressure. The residue was shaken with 150 mL of water, 24 mL of concentrated $H_3O^+Cl^-$, and 500 mL of Et_2O. The ether layer was washed with brine and extracted successively with three 800-mL portions of a solution of 150 g of NaOH in 3 L of H_2O. The alkaline solution was washed with 500 mL of Et_2O and acidified with 400 mL of concentrated $H_3O^+Cl^-$. The aqueous mixture was extracted with 1.5 L of EtOAc. The organic layer was washed with two 500-mL portions of brine, dried, and decolorized with 12.5 g of activated carbon. The solvent was evaporated under reduced pressure to give 37.4 g (72%) of **15** as a glass, suitable for further reactions. A small sample was fractionally (molecularly) distilled with the differential subliming apparatus at 300–350 °C (0.1 mm) to give **15** as a glass with transition temperature 63–100 °C: MS, M^+ 334; tlc, silica gel 60F-254 (E. Merck) precoated plate, R_f 0.19 ($ClCH_2CH_2Cl$); ^1H NMR ($CDCl_3$, 100 MHz) δ 2.34 (s, 6 H, $ArCH_3$), 2.41 (s, 3 H, $ArCH_3$), 3.33 (s, 3 H, OCH_3), 6.14 (s, 2 H, OH), 6.94 (d, J = 8.0 Hz, 2 H, ArH), 7.11 (br s, 4 H, ArH), 7.19 (s, 2 H, ArH). Anal. ($C_{22}H_{22}O_3$) C, H.

3,3″-Dibromo-2′-methoxy-5,5′,5″-trimethyl[1,1′:3′,1″-terphenyl]-2,2″-diol (16), BrAhAAhBr. Application of procedure A to 35.5 g (0.106 mol) of crude HAhAAhH (**15**) and 37.3 g (0.233 mol) of Br_2 gave 49.8 g of crude **16**, which was dissolved in 200 mL of CH_2Cl_2. Hexane (350 mL) was added, and the resulting solution was evaporated under reduced pressure until crystals appeared. The mixture, after standing at 25 °C for 24 h, was filtered, and the product was washed with hexane to give

(23) Lein, G. M.; Cram, D. J. *J. Chem. Soc., Chem. Commun.* **1982**, 301–304.

(24) We thank Dr. K. Koenig for first preparing this compound.

45.8 g (88%) of **16**, mp 174–176 °C. A small sample was recrystallized from EtOAc to give **16**, mp 176–177 °C: MS, M^+ 490 (^{79}Br); TLC (silica gel F-254, E. Merck, precoated plate), R_f 0.69 ($ClCH_2CH_2Cl$); ^1H NMR ($CDCl_3$, 100 MHz) δ 2.32 (s, 6 H, $ArCH_3$), 2.39 (s, 3 H, $ArCH_3$), 3.30 (s, 3 H, OCH_3), 6.48 (s, 2 H, OH), 7.10 (br s, 2 H, ArH), 7.16 (s, 2 H, ArH), 7.37 (br s, 2 H, ArH). Anal. ($C_{22}H_{20}O_3Br_2$) C, H, Br.

4,10-Dibromo-7,8-dihydro-19-methoxy-2,12,16-trimethyl-18,14-metheno-6*H*,14*H*-dibenzo[*f*,*m*][1,5]dioxacyclotetradecin (20). A mixture of 10.0 g (20.3 mmol) of BrAhAAhBr (**16**), KI (10.4 g, 62.9 mmol), anhydrous K_2CO_3 (8.42 g, 60.9 mmol), acetone (reagent grade, 1 L), and $Br(CH_2)_3Br$ (6.15 g, 30.5 mmol) was refluxed under dry N_2 with stirring in darkness for 10 h. The solvent was evaporated under vacuum and the residue triturated with 200 mL of boiling CH_2Cl_2 and decolorized with 2.0 g of activated charcoal. The filtrate was concentrated to about 65 mL under reduced pressure, and 270 mL of CH_3OH was added. The CH_2Cl_2 was distilled from the solution at atmospheric pressure, and the resulting solution was allowed to stand at 25 °C for 24 h. The crystals that separated were recrystallized from CH_3OH–CH_2Cl_2 to give 4.8 g (44%) of **20**, mp 184–186.5 °C; TLC (silica gel 60F-254, precoated, E. Merck), R_f 0.42 $ClCH_2CH_2Cl$, 0.45 (hexane–EtOAc (9:1)). An analytical sample was prepared by recrystallization from CH_2Cl_2–EtOH, mp 186–188 °C: MS, M^+ 530 (^{79}Br); ^1H NMR ($CDCl_3$ 100 MHz) δ 1.6–1.8 (m, 1 H, CH_2), 2.1–2.3 (m, 1 H, CH_2), 2.34 (s, 3 H, $ArCH_3$), 2.37 (s, 6 H, $ArCH_3$), 3.28 (s, 3 H, OCH_3), 3.49 (t, J = 8.6 Hz, 2 H, CH_2), 3.97 (m, 2 H, CH_2), 6.98 (s, 2 H, ArH), 7.20 (br s, 2 H, ArH), 7.36 (br s, 2 H, ArH). Anal. ($C_{25}H_{24}O_3Br_2$) C, H, Br.

4,12-Dibromo-6,7,9,10-tetrahydro-21-methoxy-2,14,18-trimethyl-20,16-metheno-16*H*-dibenzo[*h*,*o*][1,4,7]trioxocyclohexadecin (21). A mixture of 10.0 g (20.3 mmol) of BrAhAAhBr (**16**), 8.4 g (23.5 mmol) of TsOEOEOTs, 500 mL of reagent grade THF, 5 mL of H_2O, and 2.7 g (41 mmol) of KOH (~85%) was heated with stirring at reflux for 53 h, and the solvent was evaporated under reduced pressure. The residue was triturated well with 250 mL of CH_2Cl_2, and the resulting total mixture was passed through a short column of 40 g of silica gel (E. Merck) with 300 mL of CH_2Cl_2–Et_2O (9:1) as the mobile phase. The oil thus obtained was crystallized from 100 mL of EtOH to give 9.6 g (84%) of **21**, mp 170–173 °C. A small sample was recrystallized from CH_2Cl_2–EtOH to give white leaflets: mp 175–176.5 °C; MS, M^+ 560 (^{79}Br); ^1H NMR ($CDCl_3$, 100 MHz) δ 2.33 (s, 6 H, $ArCH_3$), 2.37 (s, 3 H, $ArCH_3$), 3.10 (s, 3 H, OCH_3), 3.4–4.1 (m, 8 H, CH_2), 7.03 (s, 2 H, ArH), 7.04 (br s, 2 H, ArH), 7.37 (br s, 2 H, ArH). Anal. ($C_{26}H_{26}O_4Br_2$) C, H, Br.

3,3″-Dibromo-2,2″-dihydroxy-5′,5″-dimethyl[1,1′:3′,1″-terphenyl] (13), BrAhPAhBr.[24] Under very dry conditions under nitrogen the Grignard reagent was prepared in the usual way from 2-bromo-5-methylanisole (21.0 g, 0.104 mol) and 2.8 g (0.094 mol) of triply sublimed Mg in 50 mL of dry THF (4 h reaction period). The resulting solution was added over a 10-min period under N_2 to a stirred solution of 10 g (0.0424 mol) of 1,3-dibromobenzene and 0.6 g (0.9 mmol) of $NiCl_2[P(C_6H_5)_3]_2$ in 30 mL of dry THF. An exotherm was observed, and after it subsided the solution was heated to reflux for 18 h. The solution was cooled to 25 °C, and 2 mL of water was added. The solvent was evaporated under reduced pressure, the residue was dissolved in 200 mL of CH_2Cl_2, and the resulting solution was washed several times with water. The organic layer was dried, and the solvent was evaporated under reduced pressure. The residue was chromatographed on a silica gel column (2.5 by 15 in) with first 3 L of CCl_4 as the mobile phase, and then CH_2Cl_2–CCl_4 (1:9) to produce **12** (HAPAH) as an oil: TLC (silica gel, CCl_4) $R_f \simeq 0.3$; MS, M^+ 318; ^1H NMR (100 MHz, $CDCl_3$) δ 2.22 (s, 6 H, $ArCH_3$), 3.58 (s, 6 H, OCH_3), 6.69 (d, J = 8 Hz, 2 H), 6.95 (d of d, J= 8, 2 Hz, 2 H, ArH), 7.10 (d, J = 2 Hz, 2 H, ArH), 7.40 (m, 3 H, ArH), 7.63 (br s, 1 H, ArH).

This compound (10 g, 0.0314) without further purification or characterization was dissolved in 200 mL of reagent grade CH_2Cl_2, the solution was cooled to −78 °C, and 6 mL (0.0628 mol) of BBr_3 was added in two portions. The solution was allowed to warm slowly to 25 °C, where it was stirred for 3 h. Water was added until gas evolution ceased. The mixture was strongly acidified with concentrated $H_3O^+Cl^-$, and the aqueous layer was extracted several times with CH_2Cl_2. The combined organic extracts were dried, and the solvent was evaporated under reduced pressure to give 9.9 g of crude HAhPAhH: MS, M^+ 290; ^1H NMR (100 MHz) δ 2.27 (s, 6 H, $ArCH_3$), 5.14 (br s, 2 H, OH), 6.90 (m, 6 H, ArH), 7.45 (m, 3 H, ArH), 7.58 (m, 1 H, ArH). This compound was used directly in the next step without further characterization.

Compound HAhPAhH (9.8 g, ~0.3 mol) was brominated with 10 g of Br_2 by procedure A to give 13.7 g (~0.3 mol) of crude BrAhPAhBr (**13**) as an oil (90%). An analytical sample was prepared by crystallizing the compound from $CHCl_3$–$(CH_3)_4Si$ at 0 °C to give **13** as needles, mp 159–161 °C: MS, M^+ 448; ^1H NMR (100 MHz) δ 2.23 (s, 6 H, $ArCH_3$), 5.38 (br s, 2 H, OH), 7.00 (d, J = 1 Hz, 2 H, ArH), 7.20 (d, J = 1 Hz, 2 H, ArH), 7.41 (m, 3 H, ArH), 7.62 (br s, 1 H, ArH). Anal. ($C_{20}H_{16}Br_2O_2$) C, H.

3′,3″-Dibromo-2,2″-dimethoxy-5,5″-dimethyl[1,1′:3′,1″-terphenyl] (14), BrAPABr.[24] Application of procedure B to 13.5 g (0.03 mol) of BrAhPAhBr (**13**) provided 13.5 g (~95%) of **14** as a solid. A small sample was recrystallized from cyclohexane at 0 °C to give **14**, mp 140–141 °C: MS, M^+ 476; ^1H NMR ($CDCl_3$, 100 MHz) δ 2.31 (s, 6 H, $ArCH_3$), 3.44 (s, 6 H, OCH_3), 7.09 (d, J = 2 Hz, 2 H, ArH), 7.33 (d, J = 2 Hz, 2 H, ArH), 7.48 (m, 3 H, ArH), 7.71 (br s, 1 H, ArH). Anal. ($C_{22}H_{20}Br_2O_2$) C, H.

Conversion of BrAAABr (11) to 31,32,33,34,35,36-Hexamethoxy-4,9,14,19,24,29-hexamethylheptacyclo[25.3.1.1^{2,6}.1^{7,11}.1^{12,16}.1^{17,21}.1^{22,26}]-hexatriaconta-1(31),2,4,6(36),7,9,11(35),12,14,16(34),17,19,21-(33),22,24,26(32),27,29-octadecaene·Lithium Chloride (1·LiCl), A-(AA)$_2$A·LiCl. Procedure C. To a solution of 4.9 g (9.4 mmol) of dry BrAAABr (**11**) in 100 mL of dry THF (freshly distilled from sodium benzophenone ketyl) stirred at −78 °C under argon was added 22 mL of a 1.3 M solution of *sec*-butyllithium in cyclohexane (28.6 mmol). The mixture was stirred for 10 min and then cannulated into a vigorously refluxing solution of 15 g (42.6 mmol) of dry $Fe(acac)_3$ dissolved in 1.7 L of dry benzene under argon. The resulting mixture was refluxed for 45 min. The resulting suspension of heavy red precipitate was cooled and stirred for 10 h with 600 mL of 2 N hydrochloric acid containing 7.0 g of $FeCl_3·6H_2O$ at 25 °C. The organic solvents were evaporated under reduced pressure, and the suspension was collected, washed well with water, and dried under vacuum at 25 °C. A boiling suspension of this material in 100 mL of Et_2O was concentrated to 75 mL and filtered, and the yellow solid was dissolved in 300 mL of CH_2Cl_2. This solution was vigorously stirred successively with two 600-mL portions of a 0.2 M LiCl solution saturated with EDTA and finally with deionized water. The organic layer was evaporated under reduced pressure to a 100-mL volume, 100 mL of toluene was added, and the mixture was evaporated under reduced pressure until crystals appeared (~100 mL volume). The mixture was cooled to 25 °C, and the product was collected, washed with toluene, and dried to give 1.0 g (28%) of **1**·LiCl as a white solid, mp >400 °C. Table III provides ^1H NMR data. The MS (220 °C inlet) gave a base peak for $A(AA)_2A^-Li^+$ at 712 and a substantial peak at 706 for $A(AA)_2Ah$. Anal. Calcd for $C_{48}H_{48}O_6·LiCl$: C, 75.53; H, 6.34; Cl, 4.64. Found: C, 75.34; H, 6.28; Cl, 4.75.

Complex $A(AA)_2A·LiFeCl_4$ (**1**·$LiFeCl_4$), the yellow solid remaining after the ether treatment (see above), was characterized in some runs. It was purified by dissolving 0.233 g of crude product in CH_2Cl_2 (52 mL) and adding 34 mL of glacial AcOH. The resulting greenish-yellow solution was evaporated under reduced pressure until crystals appeared. They were collected, washed successively with benzene and pentane, and dried to give 0.216 g of **1**·$LiFeCl_4$ as brilliant yellow needles, mp >400 °C. Anal. Calcd for $C_{48}H_{48}O_6·LiFeCl_4$: C, 62.29; H, 5.23; Cl, 15.32. Found: C, 62.27; H, 5.30; Cl, 15.17.

Complex $A(AA)_2A·LiClO_4$ (**1**·$LiClO_4$) was prepared by shaking a solution of 0.100 g of **1**·$LiFeCl_4$ in 80 mL of CH_2Cl_2 (reagent grade) successively with a mixture of 100 mL of a saturated aqueous EDTA solution and 20 mL of a solution of 63 mmol of $LiClO_4$ in deionized water, with a mixture of 50 mL of the EDTA and 50 mL of the $LiClO_4$ solution, and finally with 100 mL of deionized water. The organic layer without drying was evaporated to dryness under vacuum. The residue was recrystallized from CH_2Cl_2–$C_6H_5CH_3$ to give 0.079 g (88%) of **1**·$LiClO_4$, darkens without melting at 320–400 °C. Anal. Calcd for $C_{48}H_{48}O_{10}·LiCl$: C, 69.69; H, 5.85; Cl, 4.29. Found: C, 69.80; H, 5.81; Cl, 4.34.

In successive preparations of $A(AA)_6A·LiCl$ from **11** by procedure C, yields between 27 and 37% were obtained. Substitution of *n*-butyllithium for *sec*-butyllithium reduced the yield to 20%.

Application of procedure C to 3.4 g (12.1 mmol) of 2,6-dibromo-4-methylanisole[13a] in 110 mL of THF, 24 mL (31.2 mmol) of a 1.3 M *sec*-butyllithium solution in cyclohexane, and 16 g (45.5 mmol) of $Fe(acac)_3$ in 1.6 L of benzene gave 0.044 g (2.9%) of **1**·LiCl.

Application of procedure C to 4.0 g (7.7 mmol) of BrAABr[25] in 125 mL of THF, 24 mL (31.2 mmol) of 1.317 M *sec*-butyllithium in cyclohexane, and 15 g (42.6 mmol) of $Fe(acac)_3$ in 1.8 L of benzene gave 0.190 g (7.5%) of **1**·LiCl.

Procedure C could not be applied to $Br(A)_6Br$ (**19**) because of the insolubility of the derived dilithium salt in THF. When a similar procedure was used with *n*-butyllithium, and the gelatinous dilithium de-

(25) Plummerer, R.; Pullfarcken, H.; Schopflocher, P. *Chem. Ber.* **1925**, *58*, 1808–1820.

(26) Helgeson, R. C.; Weisman, G. R.; Toner, J. L.; Tarnowski, T. L.; Chao, Y.; Mayer, J. M.; Cram, D. J. *J. Am. Chem. Soc.* **1979**, *101*, 4928–4941.

rivative was poured with some difficulty and exposure to moisture into the benzene–$Fe(acac)_3$ solution, an 18% yield of **1**·LiCl was obtained.

Conversion of HAAAH (10) to $A(AA)_2A$·LiCl (1·LiCl). A solution of 1.15 mL of *tert*-butyl bromide (1.37 g, 0.01 mol distilled from K_2CO_3 under argon) in 100 mL of Et_2O (freshly distilled from sodium benzophenone ketyl) prepared under dry conditions was stirred under argon. A solution of *n*-butyllithium in hexane (7.4 mL, 2.59 M, 0.019 mol) was added via syringe through a septum cap. The mixture was stirred for 15 min, and HAAAH[13b] (**10**, 1.81 g, 0.005 mol) was added followed by 7.8 mL of *n*-butyllithium in hexane (2.59 M, 0.020 mol). The reaction mixture was heated to reflux and stirred for 3.5 h, after which the hot heterogenous mixture was cannulated by means of a double-ended needle into a solution of 13.6 g (0.0385 mol) of dry $Fe(acac)_3$ vigorously stirred in 1 L of boiling benzene (dried over activated 4 Å molecular sieves) under an argon atmosphere. The ether distilled from the reaction mixture as the addition proceeded and was allowed to escape for 1.5 h. Product, **1**·$LiFeCl_4$, was isolated as in procedure C (20.5%). It was finally converted to **1**·LiCl to give 0.32 g (17%) of **1**·LiCl, identical in all respects (^1H NMR and MS) with authentic material.

Conversion of $A(AA)_2A$·LiCl to 31,32,33,34,35,36-Hexamethoxy-4,9,14,19,24,29-hexamethylheptacyclo[25.3.1.1^{2,6}.1^{7,11}.1^{12,16}.1^{17,21}.1^{22,26}]-hexatriaconta-1(31),2,4,6(36),7,9,11(35),12,14,16(34),17,19,21-(33),22,24,26(32),27,29-octadecaene (1), $A(AA)_2A$. Procedure D. A Pyrex tube containing 0.100 g (0.13 mmol) of **1**·LiCl was suspended in 15 mL of CH_3OH–H_2O (1:4) and degassed (freeze–thaw cycles under vacuum) and sealed at high vacuum at −78 °C. The bottom end of the tube up to the miniscus was inserted into an oil bath maintained at 125 °C (the liquid refluxed, the part of the tube exposed to the air acting as a condenser) for 20 days. (Higher temperatures generate more $A(AA)_2A^-Li^+$ which lowers the yield.) The physical appearance of the white solid changed to a fine suspension as the complex dissolved and the free host crystallized. The suspension was cooled to 25 °C, filtered, washed with CH_3OH, dried under vacuum, and recrystallized from $CHCl_3$–EtOAc to give 0.079 g (84%) of **1** as white granules, mp >360 °C; MS, M^+ 720 (base peak) (see Table III for ^1H NMR). Anal. Calcd for $C_{48}H_{48}O_6$: C, 79.97; H, 6.71. Found: C, 80.18: H, 6.71.

31,32,33,34,35-Pentamethoxy-9,14,19,24,29-pentamethylheptacyclo-[25.3.1.1^{2,6}.1^{7,11}.1^{12,16}.1^{17,21}.1^{22,26}]hexatriaconta-1(31),2,4,6(36),7,9,11-(35),12,14,16(34),17,19,21(33),22,24,26(32),27,29-octadecaene (2) or $A(AA)_2P$ and 31,32,34,35-Tetramethoxy-9,14,24,29-tetramethyl-heptacyclo[25.3.1.1^{2,6}.1^{7,11}.1^{12,16}.1^{17,21}.1^{22,26}]hexatriaconta-1(31),2,4,6-(36),7,9,11(35),12,14,16(34),17,19,21(33),22,24,26(32),27,29-octade-caene (3) or $P(AA)_2P$. Cyclization procedure C was applied to 9.0 g (18.9 mmol) of BrAPABr (**14**) and 2.5 g (4.8 mmol) of BrAAABr (**11**) in 150 mL of THF, 50 mL of *sec*-butyllithium (1.42 M, cyclohexane), and 1.8 L of benzene containing 32 g (90.7 mmol) of $Fe(acac)_3$. The Et_2O filtrate from the trituration of the solid product mixture was evaporated and the residue chromatographed on 100 g of silica gel (CH_2Cl_2–Et_2O mixtures as mobile phase) to give 0.130 g of $A(AA)_2P$ (**2**). The ether–insoluble material, 1.4 g, was stirred with 150 mL of CH_2Cl_2 (8 h) to give 0.70 g of $P(AA)_2P$ (**3**) and a filtrate containing **2**, **3**, and **1**·$LiFeCl_4$. The filtrate was twice extracted with 0.2 N LiCl in water saturated with EDTA and evaporated, and the residue was recrystallized from toluene (100 mL) to give 0.165 g (9%) of **1**·LiCl. The material in the filtrate was chromatographed on 75 g of silica gel (CH_2Cl_2–Et_2O mixtures as the mobile phase) to give 0.20 g of **3** and 0.13 g of **2**. The combined portions of **2** were recrystallized from CH_2Cl_2–EtOH to give 0.190 g (6%) of **2**, mp 324–326 °C: MS (70 eV, 230 °C) M^+ 676; ^1H NMR see Table III. Anal. Calcd for $C_{46}H_{44}O_5$: C, 81.63; H, 6.55. Found: C, 81.59; H, 6.42. The combined portions of **3** (0.90 g) were recrystallized from $CHCl_3$–C_6H_6 to give 0.72 g (12%) of **3**, mp >360 °C: MS, M^+ 632; ^1H NMR, see Table III. Anal. Calcd for $C_{44}H_{40}O_4$: C, 83.52; H, 6.34. Found: C, 83.57; H, 6.36.

Application of procedure C to 6.0 g (12.6 mmol) of BrAPABr (**14**), (in 150 mL of THF) 24 mL (31.2 mmol) of 1.3 M *sec*-butyllithium in cyclohexane, and 19 g (54 mmol) of $Fe(acac)_3$ in 1.8 L of benzene gave 0.50 g of Et_2O–insoluble material which was recrystallized from *p*-xylene to give 0.35 g of $P(AA)_2P$ (3 mp >360 °C). The material in the filtrates was chromatographed on 150 g of silica gel in benzene. Product was eluted with 2 L of benzene to give 0.170 g of additional **3**, total yield 13%. This material was identical in all respects (^1H NMR and MS) with the analytical sample prepared above.

11,12,24,25-Tetrahydro-28,34-dimethoxy-3,6,16,19,31,37-hexa-methyl-1,21[1′,3′]:8,14[1″,3″]-dibenzeno-10*H*,23*H*-tetrabenzo[*f*,*h*,*o*,-*q*][1,5,10,14]tetraoxacyclooctadecin (4) or $[B(A)(M_3)B]_2$, 4·$LiFeCl_4$ and 4·LiCl. Procedure C (modified) was applied to 3.0 g (5.64 mmol) of $BrB(A)(M_3)BBr$ (**20**) in 60 mL of THF, 5.2 mL (11.4 mmol) of a 2.2 M *n*-butyllithium solution in hexane, and 6 g (17.0 mmol) of $Fe(acac)_3$ in 30 mL of freshly distilled (from sodium benzophenone ketyl) THF. The organometallic was pushed with N_2 pressure from the flask in which it was prepared through a 1.5 mm (outer diameter) needle, 60 cm in length, through a septum cap into the refluxing $Fe(acac)_3$ solution in 4 min. The resulting stirred mixture was refluxed for 1 h under N_2. The residue from the Et_2O wash was 0.372 g (13.9%) of **4**·$LiFeCl_4$. This material was dissolved in 160 mL of CH_2Cl_2, and 75 mL of glacial AcOH was added. The resulting greenish-yellow solution was evaporated under reduced pressure until crystals appeared. They were collected, washed with benzene and pentane, and dried to give canary yellow needles, 0.334 g (12.9%), mp >400 °C. Anal. Calcd for $C_{50}H_{48}O_6$·$LiFeCl_4$: C, 63.25; H, 5.10; Cl, 14.93. Found: C, 63.15; H, 5.06; Cl, 15.03.

A CH_2Cl_2 solution of this complex, $[B(A)(M_3)B]_2$·$LiFeCl_4$ (**4**·$LiFeCl_4$), was anion exchanged as in procedure C to produce $[B(A)(M_3)B]_2$·LiCl (**4**·LiCl) in 91% yield, mp 110–400 °C (slow decomposition without melting), ^1H NMR (see Table III). Anal. Calcd for $C_{50}H_{48}O_6$·LiCl: C, 76.26; H, 6.06; Cl, 4.50. Found: C, 76.10; H, 6.01; Cl, 4.48.

The free host, $[B(A)(M_3)B]_2$ (**4**), was prepared as follows. Water (40 mL) was added to a clear solution of **4**·LiCl in 10 mL of reagent grade pyridine, and the resulting white suspension was refluxed for 20 min under an N_2 atmosphere. During this period, the complex went into solution and decomplexed material, which is much less soluble in the medium, crystallized. This material was filtered, washed with water, and dried to give crude **4**, 0.118 g (62%). This material was recrystallized from CH_2Cl_2–EtOH to produce 0.104 g (55%) of **4** as fine white crystals, mp ~360 °C dec: MS, M^+ 744 (base peak); ^1H NMR, see Table III. Anal. Calcd for $C_{50}H_{48}O_6$: C, 80.62; H, 6.49. Found: C, 80.77; H, 6.41.

10,11,13,14,25,26,28,29-Octahydro-32,38-dimethoxy-3,6,18,21,35,41-hexamethyl-1,23[1′,3′]:8,16[1″,3″]-dibenzenotetrabenzo[*h*,*j*,*s*,*u*]-[1,4,7,12,15,18]hexaoxacyclododecosin (5) or $[B(A)(EOE)B]_2$, 5·LiCl, and 5·NaBr. Procedure C (modified as in the preparation of **4**) was applied to 1.0 g (1.78 mmol) of BrB(A)(EOE)BBr (**21**) in 20 mL of dry THF, 2.0 equiv of *n*-butyllithium, and 1.88 g (5.34 mmol) of $Fe(acac)_3$ in 10 mL of dry THF. The yellow crystalline powder from the ether wash was anion exchanged as in procedure C to give **5**·LiCl, 45 mg (6%), mp > 300 °C; ^1H NMR, see Table III. Anal. Calcd for $C_{52}H_{52}O_8$·LiCl: C, 73.70; H, 6.19; Cl, 4.18. Found: C, 73.68; H, 5.92; Cl, 4.07.

The free host, $[B(A)(EOE)B]_2$ (**5**), was prepared by procedure D. A Pyrex tube containing 70 mg of **5**·LiCl was mixed with 15 mL of CH_3OH–H_2O (1:4), and the mixture was refluxed at 130 °C for 4 days. The suspension was cooled to 25 °C, and the suspension was collected, washed with water, dried, and recrystallized from CH_2Cl_2–EtOH to give 48 mg (79%) of **5** as a white solid, mp 306–310 °C dec: MS (inlet, 230 °C) M^+ 804; ^1H NMR, see Table III. Anal. Calcd for $C_{52}H_{52}O_8$: C, 77.59; H, 6.51. Found: C, 77.30; H, 6.35.

31-Hydroxy-32,33,34,35,36-pentamethoxy-4,9,14,19,24,29-hexa-methylheptacyclo[25.3.1.1^{2,6}.1^{7,11}.1^{12,16}.1^{17,21}.1^{22,26}]hexatriaconta-1-(31),2,4,6(36),7,9,11(35),12,14,16(34),17,19,21(33),22,24,26-(32),27,29-octadecaene (6) or $A(AA)_2Ah$. A clear solution of 200 mg of $A(AA)_2A$·LiCl (**1**·LiCl) in 20 mL of reagent grade pyridine–deionized water (6:1) was divided into equal parts, degassed by freeze–thaw cycles in two Pyrex tubes (2.5 by 9 cm), and sealed under vacuum. The liquid part of the tubes was immersed in an oil bath maintained at 200 °C for 150 min. The clear solutions gradually became cloudy, and precipitates formed in each tube. The tubes were cooled, and the solid was collected, washed well with water, and dried to give 163 mg of a 1:1 mixture of (^1H NMR spectral analysis) $A(AA)_2Ah$ (**6**) and $A(AA)_2A^-Li^+$ (**24**) contaminated with a trace of **1**·LiCl. From the filtrate was recovered 14 mg (7%) of **1**·LiCl. The mixture of **6** and **24** was dissolved in 60 mL of hot, oxygen-free reagent pyridine (under N_2), and the resulting solution was added dropwise over a 7-min period to 600 mL of refluxing 6 N HCl in water (under N_2). The mixture was held at reflux for an additional 5 min and cooled to 25 °C. A fine precipitate formed. The mixture was extracted with two 200-mL portions of $CHCl_3$. To the combined extracts was added 50 mL of EtOH. The solution was evaporated under reduced pressure to a minimum volume to give tan crystals, which were triturated with 10 mL of CH_3OH. The product was washed and dried to give 125 mg (70%) of crude $A(AA)_2Ah$ (**6**) as white crystals. A small sample was recrystallized from CH_2Cl_2–AcOH to give **6** as white granules, mp 360–370 °C dec: MS, M^+ 706 (base peak); ^1H NMR, see Table III. Anal. Calcd for $C_{47}H_{46}O_6$: C, 79.86; H, 6.56. Found: C, 79.47; H, 6.33.

Conversion of $A(AA)_2Ah$ (6) to $A(AA)_2A$·NaCl (1·NaCl) (Procedure E). To a clear solution of 1.0 g (24.5 mmol) of reagent grade NaOH in 1.0 mL of deionized water under N_2 was added a colorless solution of $A(AA)_2Ah$ (**6**) (20 mg, 0.0282 mmol) dissolved in 20 mL of freshly distilled THF. The mixture was held at reflux for 20 min while being stirred vigorously under a N_2 atmosphere. During this period, the organic layer turned pale greenish yellow. To this refluxing mixture was added $(CH_3)_2SO_4$ (0.5 mL, 5.3 mmol), which discharged the color. The mixture was refluxed for 1 h and 40 mL of a 5% aqueous NaCl solution was added, and the organic solvent was evaporated under reduced pressure.

The residue was shaken with a mixture of 40 mL of 5% aqueous NaCl solution and 30 mL of $CHCl_3$. The organic layer was washed with 50 mL of deionized water. Toluene (20 mL) was added to the undried $CHCl_3$ solution, and the $CHCl_3$ was evaporated under reduced pressure to provide fine white crystals of **1**·NaCl which was dried to give **18** mg (95%) of product, mp 300–370 °C dec: MS (230 °C inlet), M^+ for $A(AA)_2Ah$ at 706 (base peak), M^+ for $A(AA)_2A^-Na^+$ at 728; ^1H NMR, see Table III. Anal. Calcd for $C_{48}H_{48}O_6$·NaCl: C, 73.98; H, 6.21; Cl, 4.55. Found: C, 73.74; H, 6.22; Cl, 4.36.

Attempted Conversion of $A(AA)_2Ah$ (6) to $A(AA)_2A$·KCl (1·KCl). Procedure E was applied to 20 mg of **6** in an experiment in which reagent grade KOH was substituted for the NaOH of procedure E. During the isolation, reagent grade KCl in deionized water was substituted for the NaCl solution of procedure E. The products obtained were 9.7 mg (44%) of $A(AA)_2A$·NaCl, 4.5 mg (22%) of $A(AA)_2Ah$, and 4.5 mg (20%) of $A(AA)_2A$. No $A(AA)_2A$·KCl was detected (^1H NMR, MS) among the products of this reaction.

Registry No. **1**·LiCl, 72446-98-1; **1**·LiBr, 72447-00-8; **1**·$LiClO_4$, 72446-99-2; **1**·$LiFeCl_4$, 72446-97-0; **1**·NaCl, 72447-01-9; **1**·NaBr, 72447-02-0; **1**·$NaSO_4CH_3$, 79111-13-0; **2**, 95839-28-4; **2**·$LiClO_4$, 95740-51-5; **2**·$NaClO_4$, 95740-53-7; **3**, 95839-29-5; **4**, 95782-47-1; **4**·LiCl, 73229-56-8; **4**·LiBr, 95763-28-3; **4**·$LiFeCl_4$, 73229-55-7; **4**·NaCl, 95763-29-4; **4**·NaBr, 95763-30-7; **5**, 95782-50-6; **5**·LiCl, 80128-40-1; **5**·LiBr, 95763-31-8; **5**·NaCl, 95763-32-9; **5**·NaBr, 95784-15-9; **6**, 72526-87-5; **7**, 51699-89-9; **8**, 79115-30-3; **9**, 71128-89-7; **10**, 71128-90-0; **11**, 95839-30-8; **12**, 95763-26-1; **13**, 95740-46-8; **14**, 95740-47-9; **15**, 73229-34-2; **16**, 73229-35-3; **17**, 95839-31-9; **18**, 95740-48-0; **19**, 73499-38-4; **20**, 73229-36-4; **21**, 73499-39-5; **22**, 73493-77-3; BrAhAhAhBr, 72542-40-6; H(A)6H, 80108-98-1; $Br(CH_2)_3Br$, 109-64-8; TsOEOEOTs, 7460-82-4; HAhPAhH, 80109-03-1; $Fe(acac)_3$, 14024-18-1; 2-bromo-5-methylanisole, 95740-49-1; 1,3-dibromobenzene, 108-36-1.

Supplementary Material Available: General experimental indicating solvent and reagent handling and equipment used; description of crystal structure data collection; purity of salts used and the extraction procedures; association constants and free energies of binding by $H(AA)_2P$ (**2**) of lithium and sodium picrates; and table of data (4 pages). Ordering information is given on any current masthead page.

Host–Guest Complexation. 36. Spherand and Lithium and Sodium Ion Complexation Rates and Equilibria[1,2]

Donald J. Cram* and George M. Lein

Contribution from the Department of Chemistry and Biochemistry, University of California at Los Angeles, Los Angeles, California 90024. *Received September 14, 1984*

Abstract: Thermodynamiic and kinetic parameters for complexation by three spherands of lithium and sodium picrates in $CDCl_3$ are reported. The hosts are composed of the following units (Chart I) bonded to one another in 18-membered-ring systems: 2,6-disubstituted 4-methylanisyl (A); 2,6-disubstituted 4-methylanisyl deuterated in the methoxy group (Ad); 2,6-disubstituted 4-methylphenol (Ah); 2,6-disubstituted 4-methyl-1-allyloxybenzene (Aa); 2,6-disubstituted 4-methylphenyloxy (B); 1,3-phenylene (P); 1,2-cyclohexano (Cy); ethylene (E); methylene (M); oxygen (O); and nitrogen (N). The orders of the letters in the line formulas indicate the orders of attachment of the units in the cyclic or bicyclic hosts. In the polycyclic hosts, transannular B units serve as the bridgeheads linked through their oxygens to M_3 or EOE units to transannular B units, at their 2-positions to A units, and at their 6-positions to either other B units (spherands) or to M units (hemispherands). In the cryptands, the nitrogen atoms act as bridgeheads. Chart II identifies the letters with the structures of the units and the structures and compound numbers with the line formulas. The hemispherands listed were useful in proving low, known concentrations of guests, while the chorand listed was used for dissolving sodium and lithium picrates in $CDCl_3$. The K_a and $-\Delta G°$ values for $[B(A)(M_3)B]_2$ (**2**) binding sodium picrate were determined at 25 °C in $CDCl_3$ saturated with D_2O by the direct picrate extraction method. The K_a values for $A(AA)_2A$ (**1**) and $[B(A)(EOE)B]_2$ (**3**) binding sodium picrate and for all three spherands binding lithium picrate could not be measured directly. Accordingly, values were obtained kinetically. Decomplexation rates for $Ad(AdAd)_2Ad$ (**1d**), $[B(Ad)(M_3)B]_2$ (**2d**), and $[B(Ad)(EOE)B]_2$ (**3d**) were prepared. With ^1H NMR techniques at three temperatures in $CDCl_3$ saturated at 25 °C with D_2O, the rate constants were determined for Li^+ or Na^+ transferring from nondeuterated to deuterated hosts. Because the reaction rate was comparable to rates of demethylation of the complex at high temperatures, only a maximum value could be placed on the rate constant for **1**·Li^+ + **1d** → **1** + **1d**·Li^+. Values for $\Delta H^‡$ and $\Delta S^‡$ for decomplexation were calculated, and decomplexation rate constants were extrapolated to 25 °C. Rate constants for $A(AA)_2A$ (**1**), $[B(A)(M_3)B]_2$ (**2**) and $[B(A)(EOE)B]_2$ (**3**) complexing sodium picrate were determined at 25 °C by following the ^1H NMR changes as guest was transferred from B[A][EOE][$(MOE)_2O$]B·NaPic (**6**·NaPic) to each of the three spherands. The complexation rate for complexing NaPic is much higher for **6** than for **1**, **2**, or **3**. The role of **6**·NaPic was to provide a preequilibrium concentration of NaPic low enough to bring the complexation rate of the spherands onto the human time scale. The complexation rate constant of **1** with LiPic was determined by competition experiments between NaPic and LiPic, which were delivered in $CDCl_3$ solutions via $Cy(OEOEO)_2Cy$·NaPic (**8**·NaPic) and **8**·LiPic. The rate constants for **2** and **3** complexing LiPic were determined by competition experiments between **1** and **2** and between **1** and **3** for LiPic. The complexation and decomplexation rate constants were used to calculate association (equilibrium) constants and free energies of complexation. The $-\Delta G°$ values (kcal mol^{-1}) for the various complexing partners are as follows: $A(AA)_2A$ (**1**) with LiPic, >23, and with NaPic, 19.2; $[B(A)(M_3)B]_2$ (**2**) with LiPic, 16.8, and with NaPic, 13.3; $[B(A)(EOE)_2B]_2$ (**3**) with LiPic, 15.9, and with NaPic, 18.7. The decomplexation rate constants of the spherand complexes vary by a factor of $>10^8$, whereas the complexation rate constants vary by a maximum factor of 16. Cryptand complex $N(EOE)_2(EOEOE)N$·LiPic (**9**·LiPic) was equilibrated in $CDCl_3$ at 25 °C with **2**, and the $-\Delta G°$ value for formation of **9**·LiPic was calculated to be 16.7 kcal mol^{-1}. Equilibration of $N(EOE)(EOEOE)_2N$·NaPic (**10**·NaPic) with **2** gave $-\Delta G°$ = 17.7 kcal mol^{-1} for formation of **10**·NaPic. The results show that when host–guest relationships are the most complementary in any given host class, the order for binding LiPic and NaPic in $CDCl_3$ saturated with D_2O at 25 °C is spherands > cryptands > hemispherands > chorands > open-chain polyethers.

In the companion paper of this series[3] are described the syntheses of spherands **1**–**5** and the crystals structures of **1**, **1**·LiCl, **1**·$NaSO_4CH_3$, **2**·$LiFeCl_4$, and **3**·LiCl. Qualitative binding studies of **1**–**4** established that they complexed only Li^+ and Na^+ de-

0002-7863/85/1507-3657$01.50/0 © 1985 American Chemical Society